REMOTE SENSING BASED METHOD FOR ESTIMATING CHLOROPHYLL CONCENTRATION IN SPINACH

By

THEODORE D. KERSTEN

Bachelor of Science

California Polytechnic State University

San Luis Obispo, California

1999

Submitted to the Faculty of the
Graduate College of the
Oklahoma State University
In partial fulfillment of
The requirements for
The Degree of
MASTER OF SCIENCE
August, 2002

REMOTE SENSING BASED METHOD FOR ESTIMATING

CHLOROPHYLL CONCENTRATION IN SPINACH

Thesis Approved:

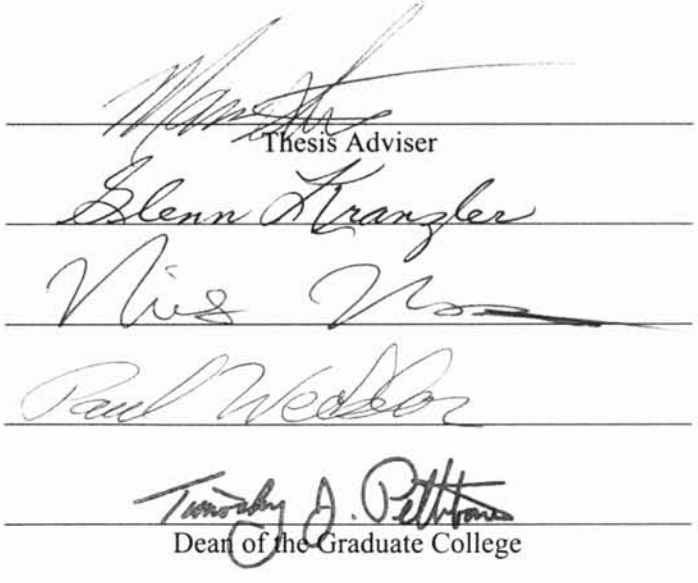

Thesis Adviser

Dean of the Graduate College

ACKNOWLEDGMENTS

I would like to express my sincere appreciation to Dr. Marvin L. Stone, my advisor, for his advice, guidance, and encouragement throughout my graduate experience. I would also like to thank my committee members, Dr. Niels Maness, Dr. Glenn Kranzler, and Dr. Paul Weckler.

I would also like to express my gratitude to Donna Chrz in Dr. Maness's laboratory for her help and patience in gathering and processing of the spinach and also to the laboratory staff of the Biosystems and Agricultural Engineering Department for their help in equipment preparation for this study.

I would like to send a special thank you to my family for their encouragement and particularly to my wife Edwina who has been a wealth of encouragement, support, and my number one fan.

TABLE OF CONTENTS

LIST OF TABLES

LIST OF FIGURES

NOMENCLATURE

A/D	Analog-to-Digital
LED	Light-Emitting Diode
NDVI	Normalized Difference Vegetative Index
NIR	Near-Infrared
%VC	Percent Vegetation Coverage
sVRT	Sensor-based variable rate technology
VRT	Variable rate technology
N	Nitrogen
Chl	Chlorophyll

Remote Sensing Based Method for Estimating Chlorophyll Concentration in Spinach

Abstract

This study investigated methods to non-destructively estimate chlorophyll concentration in the vegetative portion of spinach plants. Biomass estimates based on percent vegetation coverage data from digital images were used in conjunction with Normalized Difference Vegetative Index (NDVI) readings from two types of multi-spectral reflectance sensors to estimate chlorophyll concentration.

A field experiment was conducted to investigate the ability to use non-destructive techniques to discriminate between biomass and chlorophyll levels. Both plant density and soil fertility were varied as treatments with the expectation that the resulting chlorophyll concentrations and biomass levels would be varied

The results of the field study indicated that dry biomass was highly correlated to vegetative coverage and that NDVI measurements were highly correlated to chlorophyll content, no combined measure of NDVI and vegetative cover provided a strong measure of chlorophyll concentration. The relation between percent vegetation coverage (%VC) and dry biomass had correlations of $r^2 = 0.73$ for fall 2000 and 0.98 for spring 2001. NDVI readings from the OSU reflectance sensor correlated well with chlorophyll content ($r^2 = 0.89$) and chlorophyll concentration ($r^2 = 0.74$). Estimates of chlorophyll content were divided by estimates of dry biomass, to produce estimates of chlorophyll concentration with low correlation ($r^2 = 0.30$). Dividing the %VC by the NDVI also produced poor correlation ($r^2 = 0.39$).

An attempt was made to correlate the signals from a commercial weed detector to chlorophyll content and to chlorophyll concentration in spinach plants. The Patchen PHD 600™ detector produces a voltage output that is highly correlated to NDVI. Voltage readings of the Patchen sensor were correlated to chlorophyll content with r^2 = 0.80 and to chlorophyll concentration with $r^2 = 0.70$. Five different methods of data analysis produced correlations between processed Patchen signal and chlorophyll concentration with values ranging from $r^2 = 0.71$ to $r^2 = 0.51$.

None of the methods examined produced significant improvements in chlorophyll concentration estimates over correlations made directly from sensor calculations.

Keywords: sensor, chlorophyll, concentration, VRT, NDVI

Introduction

Both economic and environmental factors provide consistent impetus for improving agricultural practices and increasing efficiencies. Application of nitrogen fertilizer in crop production is a particular practice where opportunity exists to enhance efficiency and improve economic impact.

Determination of optimal levels for nitrogen fertilizer application is not a straight-forward process and carries significant risks. Traditionally, pre-plant nitrogen requirements have been estimated by utilizing soil samples or crop-yield levels from previous years. The determined application rate is then applied evenly to the field, and

the rate changed only between fields (Sawyer, 1994). Unfortunately, lack of soil homogeneity can lead to misapplication of nitrogen. An under-application of nitrogen may diminish crop production, while over-application can lead to negative environmental impacts including nitrogen leaching and groundwater contamination (Raun, 1998b). Therefore, a method which would allow on-the-fly in-field detection of nitrogen concentration at the time of fertilization in crop tissues could be useful in crop nitrogen management.

In order to examine field nutrient requirements, the field may be broken into smaller pieces called field elements. A field element is an area to which independent variations in crop treatments are made. Solie et al. (1996) describes a fundamental field element as the "area which provides the most precise measure of the available nutrient where the level of that nutrient changes with distance." Their research involving winter wheat suggests that variable-rate technology which utilizes field elements larger than 1.96 m^2 would not likely optimize fertilizer inputs and may potentially misapply fertilizers by utilizing a field element that is too large. Other studies indicate the application of a square meter or submeter field element may be prudent. Raun et al. (1998a) found significant differences in mobile and immobile nutrients with soil samples less than a meter apart. Using wheat, Chancellor and Goronea (1994) compared spatially modulated applications of water, nitrogen, and herbicide to blanket applications. Data were collected at one meter intervals. The greatest advantages with spatially modulated application occurred with inputs at the low and intermediate levels. The evidence also suggested significant potential for the utilization of submeter sampling and application intervals for precision application of water, N, and herbicide to maximize yield.

Variable rate technology (VRT) is a system which applies fertilizer inputs at variable levels in a site-specific fashion. VRT can be classified into two general technologies; map-based VRT and sensor based VRT or sVRT. Map-based VRT systems utilize global positioning systems (GPS) based soil type, nutrient, and yield maps as a basis for fertilizer application rate decisions. Sensor-based variable rate technology in contrast, estimates crop requirements by observing the crop's current status. In-field decisions are made by an sVRT system as it observes the plant and then applies the necessary treatment.

Map-based VRT systems have certain limitations. The conventional GPS systems used for creating maps have a resolution of approximately ± 10 m^2, and by using differential correction (DGPS) may be improved to approximately ± 1 m^2 resolution. This resolution is insufficient to reap the full benefits of VRT if the fundamental field element is in the one-meter size. The current yield monitoring systems, used to produce field yield maps, also lack the necessary resolution. Most yield monitoring systems are installed on combines with 5m or wider heads and have time delays and grain mixing associated with the harvester. These factors lead to yield monitoring systems with far from meter-level resolution. (Raun et al., 1998b).

Creating a soil nutrient map through soil sampling with meter-level resolution would require 10,000 soil samples per hectare. Soil sampling at this resolution is economically infeasible (Raun et al., 1988b). Also, once field data are gathered, processed, and a map of the field created, it is useful only for the year in which the data were collected (Stone et al., 1996a). Sawyer (1994) noted several factors limiting the effectiveness of map-based VRT systems: 1) cost of implementation (sampling, mapping,

equipment, and personnel), 2) lack of expected increase in crop yield, and 3) insufficient input savings. According to Sawyer (1994), the goal of sVRT is to avoid such traditional costs as soil sampling, chemical analysis, data management and recommendations, and to adjust application rates based on sensor measurements as the unit passes over the field.

Sensor-based variable rate systems have a finer resolution than map-based systems and avoid many of the traditional costs. (Raun et al., 1998b) The technical feasibility of sVRT systems has been demonstrated. Stone et al. (1996a) utilized sVRT in the application of nitrogen fertilizer to winter wheat. The sensor readings were at a resolution fine enough to apply the prescribed nitrogen rates to 1 m^2 field elements within the field.

The relationship between a healthy green plant canopy and energy in the visible and near-infrared electromagnetic spectrum allows the non-invasive observation of the vegetation status. Plant pigments (namely chlorophyll) have a peak absorbance in the red and blue wavelengths where the plant utilizes this energy in the photosynthesis process. In contrast, energy in the near infrared (NIR) spectrum is not utilized for photosynthesis, but scattered by the internal structure of the leaf (Thiam, 1998). The presence of nitrogen and chlorophyll are directly related. Therefore, when testing for nitrogen, a test for chlorophyll may often be used.

Molecules absorb and reflect electromagnetic energy in a characteristic fashion. The pigments in a typically healthy green plant absorb radiant energy in the blue and red portions of the visible spectrum (Jensen, 2000). Chlorophyll *a* reaches peak absorbance at 430nm and 660nm and chlorophyll *b* at 450nm and 650nm. There is a region of low absorbance (high reflectance) between these two sets of peaks in the green region of

540nm. This high absorbance of blue and red light combined with the relatively low absorbency of green light causes the leaf to appear green to the eyes. Red light is absorbed by leaf chlorophyll and is an important indicator of plant metabolism. Pinter et al. (1987) demonstrated that healthy green plants have a low reflectance (2-5%) in the visible portion of the electromagnetic spectrum, but reflect 50-60% of incident light in the NIR spectrum.

A calculated multi-band combination of specific reflectances that maximizes spectral differences in plant canopies and soils is called a vegetation index (Pinter et al., 1987). One such index is the Simple Ratio utilized by Birth and McVey (1968). The formula for the Simple Ratio is:

$$SR = \frac{NIR}{red} \tag{1}$$

NIR = near-infrared intensity (Birth and McVey used 740nm)

red = red intensity (Birth and McVey used 675nm)

An index offered by Rouse et al. (1974) to separate green vegetation from the soil background is a normalized version of the Simple Ratio formula, the Normalized Difference Vegetative Index (NDVI):

$$NDVI = \frac{I_{NIR} - I_{RED}}{I_{NIR} + I_{RED}} \tag{2}$$

I_{NIR} = incident near-infrared intensity

I_{NIR} = incident red intensity

NDVI produces a linear scale ranging from -1 to +1, with zero approximating the equivalent of no vegetation (Thiam, 1998). NDVI is based on reflected light that is heavily influenced by chlorophyll. Chlorophyll *a* content is mainly determined by

nitrogen availability (Moorby and Besford, 1983). A linear relationship has been observed between chlorophyll concentration and yield (Munden et al., 1994). NDVI has been correlated with such plant properties as leaf area index, fractional vegetation canopy, vegetative condition, biomass, nitrogen content, and nitrogen concentration (Carlson, 1997; Sembiring, 1998). Leaf area index (LAI) may range from zero to four or greater and is defined as the total of one-sided leaf area measured over an area per unit area. Fractional vegetation coverage is the fraction of a given area that is covered by vegetation in a two-dimensional view from above. NDVI increases nearly linearly with LAI and then enters an asymptotic condition where large increases in LAI bring small increases in NDVI (Carlson, 1997). Differences may be found when nearing full vegetative canopy or approximately an LAI value between 2-4.

Sembiring (1998) found NDVI to be a better predictor of plant nitrogen content than nitrogen concentration or biomass. Studies by Lukina et al. (1999, 2000) also support NDVI as a better predictor of nitrogen content than nitrogen concentration. Nitrogen content is the total mass of nitrogen present in the plant vegetation above ground in the area considered. Nitrogen concentration is the unit mass of nitrogen present per unit mass of biomass. Using winter wheat, Stone et al. (1996a) found a high correlation between nitrogen content and plant nitrogen spectral index (PNSI) in winter wheat at several different growth stages. PNSI is inversely related to NDVI. Stone et al. (1996a) demonstrated the validity of sVRT for nitrogen application through the variable application rate of nitrogen to winter wheat based on PNSI. The result was an increase in nitrogen efficiency, decreased spatial variation, and increased yield when compared to

the standard fixed application rate. Deficiencies in nitrogen may now be detected and corrected using sensor-based technology (Raun, 1998b).

Vegetative indices which are based on the light reflected from the target of interest are referred to as irradiance-based indices. Vegetative indices which measure the intensity of light reflected from the observed area as a ratio to the intensity of light striking the same area are referred to as reflectance-based indices. A sensor which utilizes only reflected light to calculate NDVI will be sensitive to changes in solar azimuth (Pinter et al., 1990). Cloud cover has been shown to have a minimal effect on ratio type vegetation indices, such as NDVI, since both the red and NIR bands are equally affected (Pinter, 1987). Changes in solar angle, however, have been found to have a significant effect on NDVI readings (Pinter, 1993).

Merritt et al. (1994) utilized reflectance readings to compensate for changes in lighting conditions by estimating the incident red and NIR light intensities from a reference surface painted with flat white paint, in addition to the red and NIR light intensities reflected from the plant vegetation. Identical photo-detector pairs were used to gather red and NIR incident and reflected light intensities. The photo-detector outputs generated from light reflected from the white plate were used to represent incident light intensities. The photo-detector output generated from red light reflected by the plant was divided by the photo-detector outputs generated from incident red light reflected from the white plate. Likewise, the photo-detector outputs generated from reflected NIR was divided by the photo-detector outputs generated from incident NIR. These reflectance values were then place into the standard NDVI formula. Merritt et al. (1994) referred to this as the NDI equation:

$$NDI = \frac{\frac{NIR_F}{NIR_R} - \frac{RED_F}{RED_R}}{\frac{NIR_F}{NIR_R} + \frac{RED_F}{RED_R}} \quad (3)$$

NIR_F = Reflected NIR light from the field sensor

NIR_R = Reflected NIR light from the reference sensor

RED_F = Reflected red light from the field sensor

RED_R = Reflected red light from the reference sensor

By dividing the reflected light by the incident light estimation, Merritt et al. (1994) utilized a reflectance-based NDVI, in contrast to the more commonly used radiance-based NDVI previously described and introduced by Rouse (1974).

A sensor conceptually similar to the one used in the study by Merritt et al. (1994) has been developed and utilized in several different Oklahoma State University (OSU) studies. This sensor has been unofficially dubbed the "OSU Plant Reflectance sensor" since the red and NIR reference readings are not taken from a white plate, but rather from a cosine corrected incident light reference sensor aimed at the sky. This method provides a simultaneous incident light reading for red and NIR solar irradiance.

At least two types of spectral-based sensors may be defined: passive and active. Passive sensors rely on the availability of incident light and may be irradiance-based or reflectance-based. An example of a passive sensor would be the OSU Plant Reflectance sensor. An active sensor is removed from dependence on incident light by producing its own light from which measurements are taken. An example of an active sensor would be the WeedSeeker™ PHD600 Manufactured by Patchen Inc. The WeedSeeker™ uses light emitting diodes (LEDs) to produce the light from which measurements are taken. Natural incident light and LED light are separated, and a voltage signal is produced which is

related to the fractions of reflected NIR and red light. This voltage is then passed through a comparator to produce a high- or low-voltage output.

One technique for estimating biomass utilizes photo imagery. Ter-Mikaelian and Parker (2000) used photo imagery to estimate the biomass of white spruce seedlings by examining a seedling side-view silhouette area. The accuracy of the imagery technique was found comparable to the traditional allometric methods using seedling basal diameter. Adamsen et al. (2000) used color digital camera images to estimate the number of lesquerella flowers in experimental plots. The pictures were manipulated to produce a binary image so the value of one represented yellow pixels (plant flowers) and a value of zero represented black pixels (non-flower picture background). A pixel count was then performed to find the percent of pixels in the image representing flowers. This method produced estimates that were highly correlated with a manual flower count with a correlation of $r^2 = 0.83$.

Lukina et al. (1999) used images from a digital camera to estimate vegetation coverage in plots of winter wheat. Nitrogen concentration, nitrogen content, dry biomass, and NDVI readings were also recorded for each plot. Images were taken with a digital red-green-blue camera and processed with Micrografx Picture Publisher® to produce a binary image where the vegetation appeared black and the soil background appeared red. From this image, the percent of black pixels in each image was calculated for each plot and used to represent the percent vegetation coverage (%VC) of each plot. Percent vegetation coverage is the percent of a given area that is covered by vegetation in a two-dimensional view from above. Percent vegetation coverage was found to have a strong relationship with NDVI ($r = 0.81$ to 0.98). NDVI, in turn, was found to have strong

relation with dry biomass (r = 0.71) and N content (r = 0.81). In a separate experiment, Lukina et al. (2000) examined the effect of row spacing, growth stage, and nitrogen rate on indirect spectral irradiance measurement in winter wheat. The study indicated percent vegetation coverage was a good predictor of other dependent variables including forage dry matter (r = 0.32 to 0.81) and N content (r = 0.42 to 0.82). The studies of Ter-Mikaelian and Parker (2000) and Lukina et al. (1999, 2000) support the hypothesis that percent vegetative coverage may be useful in estimating the biomass of a plant canopy.

Total vegetative chlorophyll content is a product of vegetative chlorophyll concentration and vegetative mass (Stone et al., 1996b). To date, the ability to non-invasively estimate the nitrogen concentration in a plant canopy has not been well demonstrated, though there has been reasonable success in non-invasively estimating the nitrogen content of plant vegetative biomass. The ability to estimate biomass using percent vegetation coverage has also been demonstrated. Since N content is a product of N concentration and biomass, and N content and biomass may be non-destructively estimated, it is reasonable to postulate N concentration may be estimated by utilizing estimates of N content and biomass.

Objective

The objective of this study was to investigate non-destructive estimation of chlorophyll concentration in spinach by using estimates of biomass and chlorophyll content. Biomass was estimated from percent vegetation coverage from pictures taken by

a digital still camera which were processed to produce pixel thresholds to represent percent vegetative cover. Chlorophyll content was estimated by using the OSU Plant Reflectance sensor and the Patchen WeedSeeker™ sensor. Chlorophyll content is the total mass of chlorophyll present in the plant vegetation above ground in the area considered. Chlorophyll concentration is the unit mass of chlorophyll present per unit of biomass.

Methods

Field plots of spinach were planted in the Fall of 2000 and Spring of 2001 at OSU's Bixby Vegetable Research Station in Bixby, Oklahoma. The variety Fidalgo was planted in the fall and San Juan in the spring. The soil was a Severn very fine sandy loam with each field having been fallow the previous year. Soil tests indicated a residual N level of nine kg ha^{-1}. Plots were irrigated with hand-moved sprinkler irrigation.

This experiment was arranged in a randomized complete block design, with four replications. Each replication had two N levels and three different plant spacings, for a total of 24 plots. Two nitrogen levels were used to obtain independent variation of biomass in the plot and nitrogen concentration in the plants. See Appendix A for plot layout.

Seeds were planted at a rate of 39 seeds to a linear meter with a prior application of Rowneet™ for weed control. Each plot was 1.5-m wide and 6-m long, with four rows spaced 0.38-m apart. Once seeds were planted, fertilizer was applied to half of the plots

in the form of ammonium nitrate at the rate of 140 kg ha^{-1} with the other half left unfertilized. In this experiment, 12 plots received ammonium nitrate at 140 kg ha^{-1}, and 12 plots received no additional fertilizer. While only a portion of each plot was to be utilized, it was prudent to plant a larger plot in case of experimental mishaps. Weed sprouts were removed by hand hoeing. When the seedlings had matured to the 5-leaf stage, the plots were hand thinned to seedling spacings of 5.1, 12.7, and 25.4 cm.

The experiment was conducted when the spinach was approximately 45 days old. At this point the spinach, which had received 140 kg ha^{-1} of ammonium nitrate and a plant spacing of 25.4 cm, had reached approximately 75% coverage in each row. The spinach, which had received no ammonium nitrate and a plant spacing of 25.4 cm, had reached approximately 40% coverage in each row. From each plot, a representative portion was selected and a frame placed over the center two rows, see Figure 6. Images were taken, and then spectral readings were recorded with the OSU sensor and the Patchen sensor. The appropriate spinach in the frame was then hand cut, sealed in a polyethylene bag, and placed on ice in a cooler until all plot samples had been collected. These samples were then transported to facilities in Stillwater for washing, freezing, lyophilization, grinding, and chlorophyll analysis.

The OSU Plant Reflectance (OSUPR) sensor is a passive sensor that measures both incident and reflected red and NIR wavelengths, thus allowing reflectance to be calculated. Reflectance is the fraction of incident light reflected by the targeted surface. A simplified diagram of this sensor may be seen in Figure 1.

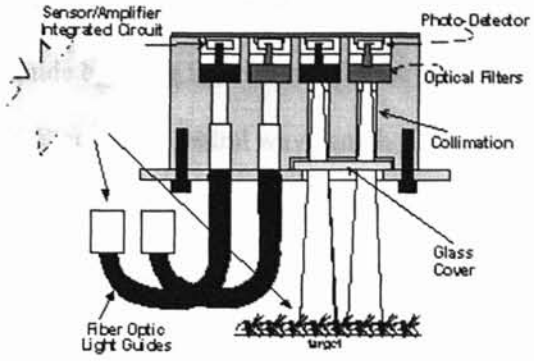

Figure 1. Simplified diagram of OSU Plant Reflectance Sensor.

In Figure 2, I_{red} represents the intensity of incident red light in the visible spectrum which strikes the target. The portion of that light which is reflected from the target is represented by R_{red} .

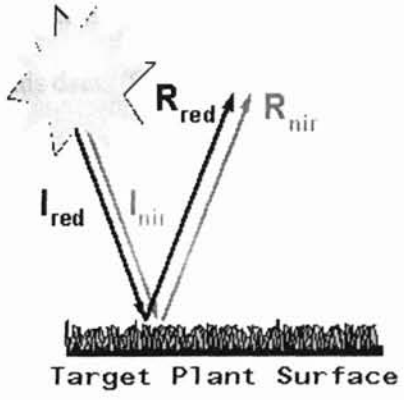

Figure 2. Incident and reflected light

The incident light detector assembly on the OSU Plant Reflectance sensor gathers the incident light. It consists of two cosine-corrected Teflon diffusers, each of which is connected to the sensor photo diode filter assembly with two 1/8" x 36" multi-strand fiber

optic light guides; one for red and one for NIR. The red and NIR wavelengths are isolated for each light guide by using interference filters. Reflected red light passes through an interference filter with a central wavelength (CWL) of 671nm $\pm$2 and a full-width half-maximum (FWHM) equal to 10nm $\pm$ 2. Reflected NIR light passes through an interference filter with a CWL of 780nm $\pm$ 2 and a FWHM equal to 10nm + 2. The photo-detectors are Burr-Brown OPT-210 photo-detectors and consist of a photodiode and matched transconductance amplifiers on four channels. Data from each channel are processed through a low-noise programmable gain amplifier (1, 2, 4, 8, 16, 32, and 64) and an analog multiplexer to a 16-bit A/D converter. A microcontroller converts data and sends it to a laptop via a serial port. The laptop uses a "dumb" terminal program which captures the data sent from the sensor and saves it as a text file. Information saved includes four inputs: red incident, NIR incident, red reflected, and NIR reflected. User selected gains for each of the four channels are also saved with each file. The reflectance NDVI may be calculated from this data. The analog processing elements in the sensor are fully optically isolated from the computer with noise levels on the order of 2 counts in a range of 65,535 counts (16-bit converter). The reflected and incident readings must be corrected for gain before they are used to calculate NDVI. A separate "white plate" correction factor must also be used to correct for intrinsic differences between the channels due to component and manufacturing variations. The gain correction factors (CF) obtained by measuring the reflectance of a white barium sulfate plate that has a reflectance of nearly 1.0 for the spectral range of interest. The calibration factors are shown in Table 1.

	Spectral Band	Calibration Factor
CF_{red}	Red	0.31
CF_{NIR}	NIR	0.43

Table 1. Sensor calibration factors.

The gain-corrected light intensities for each band are then calculated using the following formulas:

R_{red} = Reflected Red / $Gain_{Red\text{-}R}$
I_{red} = Incident Red / $Gain_{Red\text{-}I}$
R_{NIR} = Reflected NIR / $Gain_{NIR\text{-}R}$
I_{NIR} = Incident NIR / $Gain_{NIR\text{-}I}$

Once I_{red}, I_{NIR}, R_{red}, and R_{NIR}, are corrected for the appropriate gain values, the sensor calibration factor may be applied to obtain the red reflectance (ρ_{red}) and NIR reflectance values (ρ_{NIR}) as follows:

$$\rho_{red} = CF_{red}\left[\frac{R_{red}}{I_{red}}\right] \tag{4}$$

$$\rho_{NIR} = CF_{NIR}\left[\frac{R_{NIR}}{I_{NIR}}\right] \tag{5}$$

The reflectance based NDVI (named NDI by Merritt et al. (1994)) is calculated by using the reflectance calculations ρ_{red} and ρ_{NIR} and entering them in the standard NDVI equation as follows:

$$NDVI = \frac{\rho_{NIR} - \rho_{red}}{\rho_{NIR} - \rho_{red}} \tag{6}$$

The PHD WeedSeeker™ manufactured by Patchen Inc., of Ukiah, CA is an active sensor which produces its own light in the red and NIR energy bands by utilizing light

emitting diodes (LEDs). The LEDs are controlled with digital logic and utilize frequency modulation techniques, band-pass filtering, and phase shift detection to allow separation of the modulated LED light and the incident light (Beck, 1996). The sensor produces a voltage signal which is related to the fractions of reflected NIR and red light. This variable voltage signal is then passed through a comparator to produce a binary voltage output consisting of a high or low voltage, thus allowing it to control valves for the purpose of spot-spraying vegetation. Voltage output of the Patchen PHD before the comparator correlates well with NDVI readings from the OSU Plant Reflectance Sensor when applied on a turf target as shown in Figure 3 (Needham, 2002). Each point on this graph represents approximately ten readings and their associated error bars.

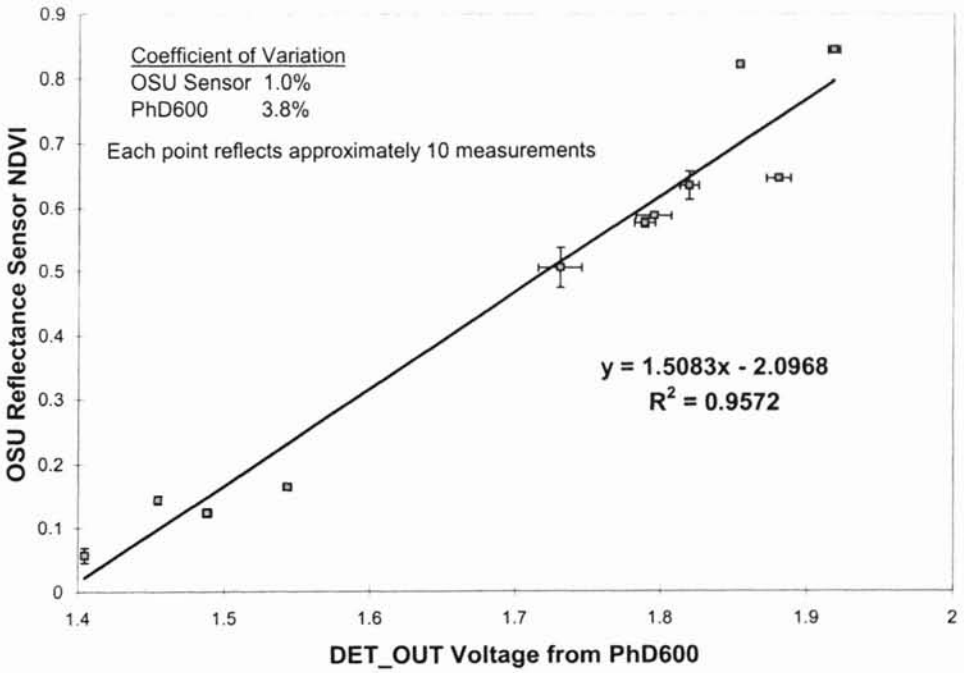

Figure 3. Calibration of Patchen PHD output voltage with reflectance NDVI from the OSU Plant Reflectance sensor (Needham, 2002).

Two different sensors were utilized in this experiment: the OSU Plant Reflectance sensor and the Patchen WeedSeeker™ PhD600 which will be referred to as the passive sensor and the active sensor respectively. Each sensor was mounted on a separate arm on a two-wheel push-cart as shown in Figures 4 and 5. This configuration allowed each sensor to extend over the plot, while casting no significant shadows on the region being observed.

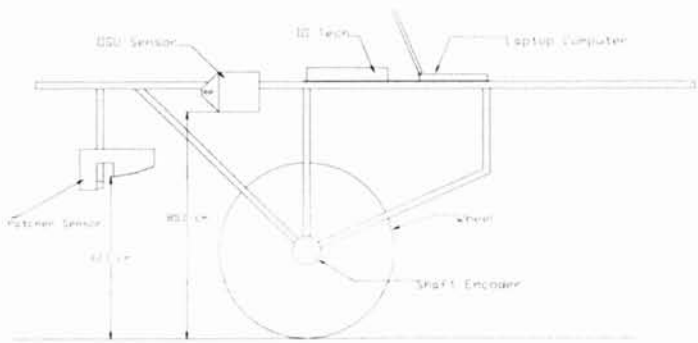

Figure 4. Side view of sensor cart.

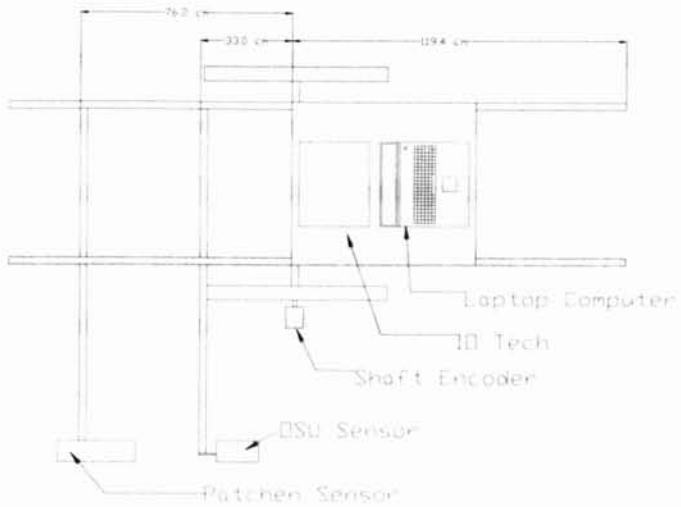

Figure 5. Top view of sensor cart.

The field-of-view of the OSU sensor at a height of one meter was 250 mm along the axis of travel and 750 mm across the axis of travel. For this experiment, the lens of the sensor was masked to 1cm x 1 cm and mounted at a height of 85 cm, which gave the sensor a view of 25.4 cm x 25.4 cm at ground level. Readings were time-base triggered at a rate of 15 Hertz. The sensor was pushed over the plot at a consistent speed, providing approximately 60 overlapping readings per plot. The Patchen sensor was mounted at a height of 61 cm with a field-of-view of 1 cm along the axis of travel and 30.5 cm across the axis of travel. The Patchen detector, a shaft encoder, and a laptop computer were connected to an IO Tech data logger which was used to digitize the signal from the Patchen detector with 12-bit resolution. The recording of readings from the Patchen were controlled by the IO Tech data logger and triggered by the shaft encoder attached to the cart wheel which provided non-overlapping readings spaced approximately one

centimeter apart. Proprietary software in the laptop was then used to move the data from the IO Tech data logger to a disk file where it was saved as a text file. The Patchen sensor, OSU sensor, and IO Tech data logger were powered by a 12-volt automotive battery. The size and spacing of the Patchen readings allowed the plot data to be treated as a series of linear images. In this study, all readings taken by the Patchen PHD sensor were of the variable voltage produced by the detector before it entered the binary comparator.

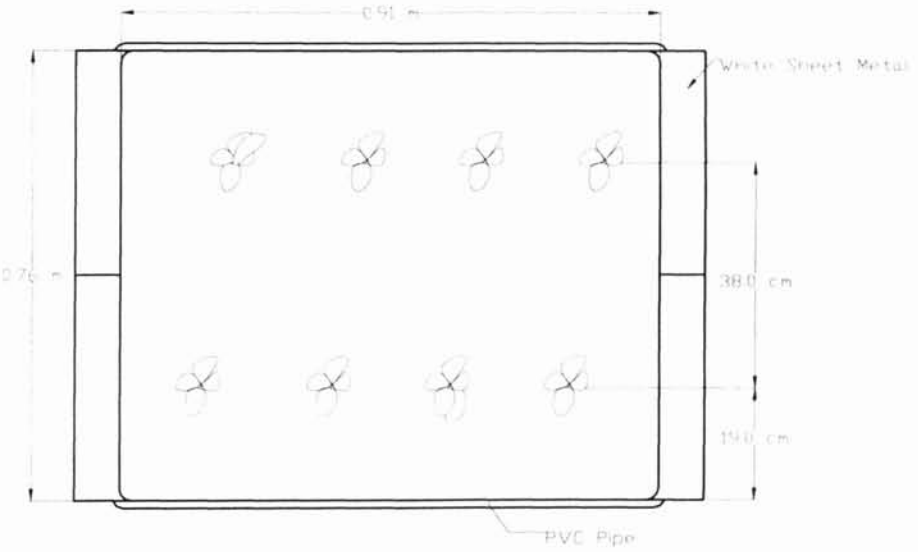

Figure 6. Drawing of plot frame in position.

A plot of known and consistent size was created by placing the plot frame over the area of interest before the measurements and pictures were taken (Figure 6). The frame was constructed of 1.27-cm (3/4") PVC pipe having a rectangular shape with inside dimensions of 0.76-m wide x 0.91-m long. Both frame ends, which lay perpendicular to the row, had a length of 0.076-m x 0.76-m white sheet metal attached

horizontally to the outer edges of the frame. These white strips created an anomaly in the sensor data that was later used to isolate the sensor readings that occurred inside the frame. Markers were also placed on each side of the frame to aid image cropping. The outer sides of the frame were painted black to minimize interaction with the sensor.

Pictures were taken with an Olympus D-360L digital camera with an image resolution of 1280 x 960 pixels and stored in JPEG format. The camera was mounted on an aluminum bar and attached to a 1.8-meter ladder at a height of 1.5 meters as shown in Figure 7. The length of the camera arm was adjusted to allow the camera to be centered over the plot when a picture was taken.

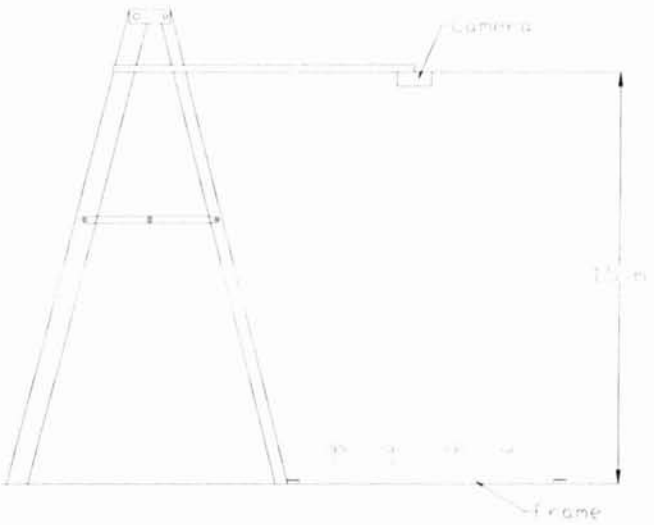

Figure 7. Ladder tripod centered over plot.

Once the frame and tripod were positioned, two images were taken and the tripod removed. The sensor cart was then positioned to take sensor readings. First the passive sensor was passed over the plot and the data saved. The active sensor was then

passed over the plot in the same direction and the readings saved. Both sensors were started and stopped outside the frame. In this way, the sensor would begin taking readings outside the frame, pass over the white sheet metal marker, over the plot, over the second white marker, and stop outside the frame. The field-of-view of the passive and active sensors limited their view to the width of one row of spinach.

Of the two rows inside the confines of the frame, one was selected to be observed by the sensors and harvested for analysis. In the fall experiment, one row was observed while both rows were harvested and analyzed. With the exception of %VC, the fall experiment was excluded from analysis, since the data being analyzed did not match the plant sample taken. The %VC analysis for fall was still useful, because the image analysis procedure could be modified to include both harvested rows. In the spring experiment, only the row which was observed by the sensors was harvested for analysis. The spinach was harvested for chemical analysis by hand clipping at ground level, with all weed sprouts removed prior to the experiment. The harvested spinach was then placed in a plastic bag, labeled, and excess air removed from the bag before it was sealed. It was then placed on crushed ice in an ice chest. Once all the samples were collected, each sample was hand sifted on a screen to remove any non-vegetative matter, weighed, re-bagged, and returned into the ice chest. In the afternoon, the samples were taken to Stillwater, Oklahoma where they were refrigerated for processing the following day. The spinach was washed, freeze dried, and analyzed for chlorophyll content using the spectrophotometric method of Inskeep and Bloom (1985).

Plot images were processed with Micrografx Picture Publisher®. Since only the image inside the plot frame was of interest, each picture was manually cropped to contain

only the image inside the plot frame. Only one of the two rows in the spring experiment was observed by the sensors. Therefore, all spring images were cropped to include only the observed row. Visible markings on the sides of the frame provided consistent reference points for cropping of the images within the frame. Consistency in image size is important for the comparison of plots on a bases of %VC. After cropping, each image was stored. A binary image was created by processing the cropped images as outlined in Table 2. Figure 8 provides image samples of the steps in Table 2.

Creation of the binary image was a process of manipulating plant and soil background in the image through a series of color manipulation techniques. Colors in the image were manipulated by changing the yellow hues to red, which turned plant material red. Color saturation was then maximized and the image split into three separate images of hue, saturation and lightness. The hue image was selected for further processing. De-speckle was applied which acted as low-pass filtering of the image. Further low-pass filtering was performed by applying image smoothing at a median four level. A threshold was then applied turning the image into a black and white binary image. A 'chroma mask' was generated and saved for the white portions, which represented plant material in the image. This mask was then applied to the original cropped picture and appeared as a rough outline of the spinach plants. This outline was adjusted where any discrepancies were observed to match the spinach outline by manually adjusting the mask. The spinach plants were now accurately outlined with the mask. The inside of the mask, which represented spinach plant, was filled with black. The outside of the mask, which represented non-spinach, was filled with white. This created a binary image where black represented spinach plant and white represented non-spinach background. A

histogram was performed on the image to produce a count of black and white pixels. This count enabled the percentage of plant-to-soil pixels to be calculated and the percent vegetation coverage to be found.

It was necessary to process the files from the passive sensor to obtain whole-plot NDVI readings. Data from the passive sensor were saved in text files. These files were imported into Excel spreadsheets and the reflectance NDVI calculated. The NDVI values were plotted to show a graph of values taken by the sensor versus position in the plot. The graph (Figure 9) shows the anomalies created by the white frame markers which denote the beginning and end boundaries of the plot frame.

Step	Description	Commands	Effect
1	Open image	<File/Open>	Figure 6, Picture I
2a	In the **Image** Menu select **Effects** option	<Image/Effects>	Dialog box displayed
2b	In the **Image** menu select **Effects**. In the **Image Efects** window select **Hue Adjustment**; move Yellow slider to Red, value=360. Click **Apply** Button.	<Image/Effects/Image Effects/Hue Adjustment>	Changes yellow hues in picture to red hues.
2c	In the **Image Effects** window select **Color Saturation** ; Move Slider to pure, value=10. Click **Apply** Button. Click **OK** Button.	<Image/Effects/Image Effects/Color Saturation>	Original Image in Original box will be changed, saturated with pure colors. Figure 6, Picture II
3a	In the **Image** menu select **Channels**, then select **HSL**. Click on the **Yes** button.	<Image/Channels/HSL> Click **Yes**	Seperates the image into three separate images. Hue, Saturation, Lightness
3b	Select the H Image.		Selects the H image for further processing commands. Figure 6,
3c	In the **Image** menu select **Effects**. In the **Image Effects** window select **Despeckle**. Click **Apply** Button.	<Image/Effects/Image Effects/Despeckle>	Removes small specks from the image. (low-pass filter)
3d	In the **Image Effects** window select **Smooth**. Click on **Median**. Set Slider to read 4. Click **Apply** Button. Click on **Threshold**. Click **Apply** Button. Click **OK** Button.	<Image/Effects/Image Effects/Smooth/Medium> ;<Image/Effects/Image Effects/Threshold>	Low-pass filters image and then changes image to binary black and white. Figure 6, Picture IV.
4a	In the **Mask** menu select **Chroma Mask**.	<Mask/Chroma Mask>	
4b	Select one **Color Select** button in the Dialog box. Point a ***drop stick*** cursor on the white part of the image (representing plant) and click the left button of the mouse. Click **OK** button in dialog box.		Chroma mask appears on the image, plant related compartments on the image are selected.
5	In **Mask** menu, select **Save Mask**. Enter name to be saved as.	<Mask/Save Mask>	Saves mask for future use.
6	In **File** Menu, select **Close All**. Select **NO** in save changes dialog box.	<File/Close All>	
7a	Open original image	<File/Open>	
7b	In **Mask** menu, select **Load Mask**. Select mask name.	<Mask/Load Mask>	
7c	Mask is imposed over original color picture. Manually adjust mask to fit plant. Resave Mask.		Figure 6, Picture V.
8a	In the button toolbar select **Color Swatch** button, select the **Black** button, click on **OK**. Select the **Fill Tools** button. Select **Fill Image** button. Click on image.		Fills inside of mask with black, representing plant mass.
8b	In the **Mask** menu select **Invert Mask**.	<Mask/Invert Mask>	
8c	In the button toolbar select **Color Swatch** button, select the **White** button, click on **OK**. Select the **Fill Tools** button. Select **Fill Image** button. Click on image.		Fills outside of mask with white, representing non-plant background. Figure 6, Picture VI.
8d	In **File** menu, select **Save As**. Enter name to safe modified file as.	<File/Save As>	
9	In **Map** menu select **Histogram**.	<Map/Histogram>	A histogram of each band is computed. Soil and plant related pixels are counted. Shadow indicates the percentage of black pixels in the image, which correspond to the vegetation.

Table 2. Image processing algorithm[1].

[1] The image processing algorithm was executed in Micrografx Picture Publisher™ and is expressed in the command language of the package.

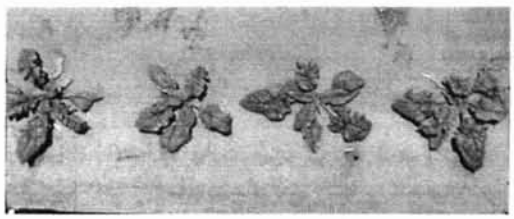

Picture I. Original Image.

Picture II. Pure color saturation image.

Picture III. Hue image.

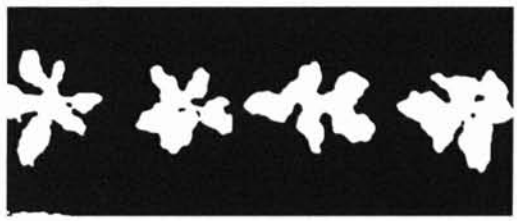

Picture IV. Thresholded image.

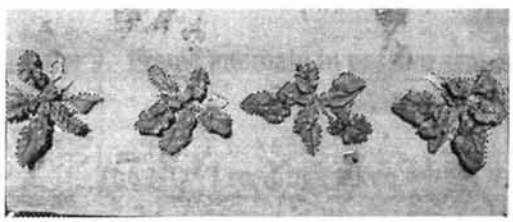

Picture V. Image with mask overlay.

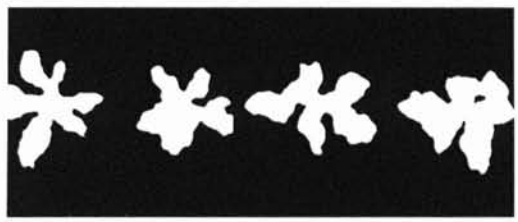

Picture VI. Finished binary image.

Figure 8. Examples of image processing steps as outlined in Table 2.

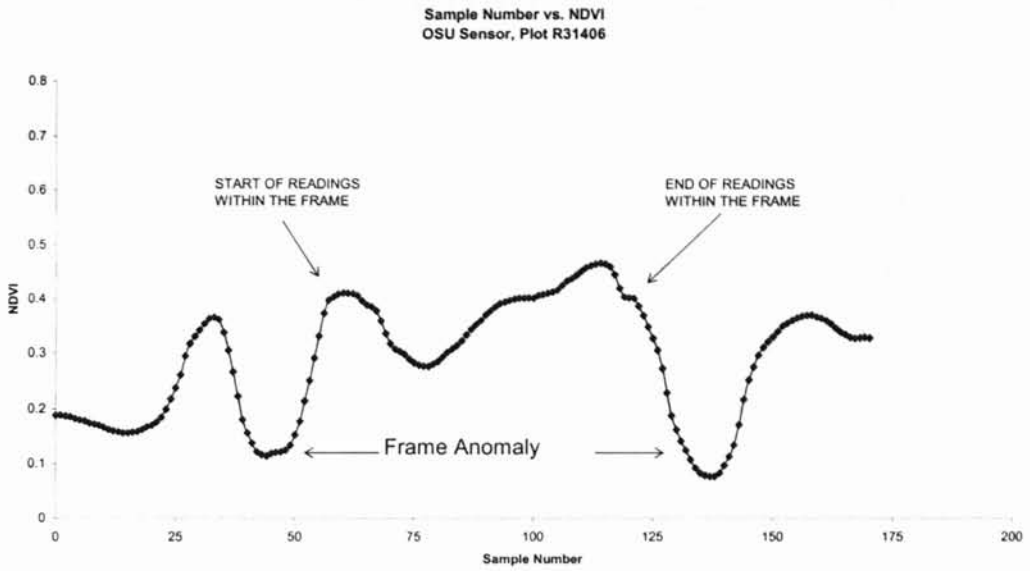

Figure 9. Frame anomaly in passive sensor data.

The NDVI readings taken within the boundaries of the plot frame, were isolated by examining the NDVI plot graph, and identifying the frame anomalies. The field-of-view for the passive sensor is 25.4 cm by 25.4 cm. The sensor reading is an average of what is observed in the field of view. As the white plate comes into view of the sensor, the NDVI reading will begin to decrease until the sensor passes. Then, the NDVI reading increases again. A dip forms in the NDVI graph, which is readily identifiable (Figure 9). These dips are created in the sensor readings at the beginning and end of the plot. Points inside the plot frame were selected by visually examining the NDVI graphs and selecting the inner point at which each white plate anomaly occurs. Data between these points were considered to be inside the plot frame. From these data, the reflectance NDVI values were calculated and averaged to produce a plot average NDVI value.

The process used to isolate the active sensor data inside the plot frame was similar to that used on the passive sensor files. The original active sensor files, which were saved in text format, were converted to Excel spreadsheets and graphs created directly from the sensor voltage readings. Points between the frame anomalies (Figure 10) were selected for analysis. The starting points were selected where the anomaly dip ended and the soil/plant readings started. The ending points were selected where the anomaly dips started and the soil/plant readings ended. Once isolated, these voltage levels were further processed. From an analysis perspective, data from the active detector represented a linear image of the plot.

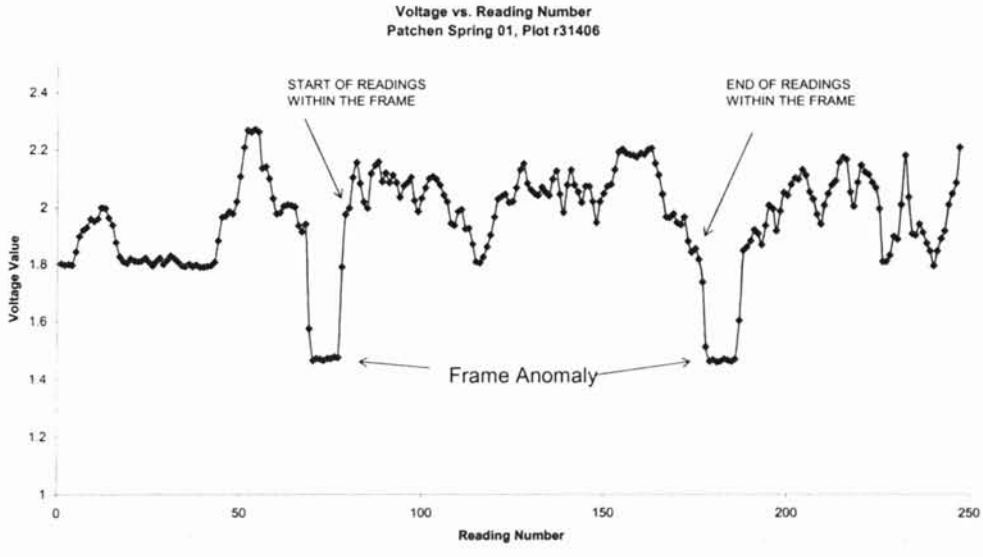

Figure 10. Frame anomaly in active sensor data.

Six different methods were used to examine the active sensor data as summarized in Table 3. Results of which may be found in Appendix C. All methods examined only the data points within the plot frame. The first method was to calculate the whole plot

average voltage that was found by averaging all data readings within the plot. The plot voltages were graphed against chlorophyll content and concentration. The second method calculated the plant plot average voltage; that is the average of all voltage readings taken while the sensor was over plant mass. This method will be referred to as the exemplary method. By examining the plot image and graph of sensor readings, it was possible to isolate readings containing plant matter from those containing no plant matter. Once separated, the number of plant data points was recorded and their average voltage calculated and recorded. This voltage was the plant plot average voltage and was graphed against chlorophyll content and concentration. The third method applied a fixed threshold to all plot readings. The threshold was adjusted to minimize the difference between the total number of data points above the threshold for all 24 plots and the exemplary method total for the 24 plots. Once the threshold was adjusted, the average voltage above the threshold was calculated for each plot and graphed against chlorophyll content and concentration. The fourth method was similar to the third, except that an individual threshold was adjusted and applied to each plot. These plot voltages were graphed against their corresponding chlorophyll concentration and chlorophyll content. The fifth and sixth methods investigated the area under the curve and its relation to chlorophyll concentration and chlorophyll content. Higher voltage readings from the sensor indicate greater presence of nitrogen. Also, because readings from the active sensor were evenly spaced, a greater number of readings above the threshold would tend to indicate more plant matter. Method five multiplied the average plot voltage above the fixed threshold by the number of points above the threshold. Method six was similar to method five, but used the threshold levels and number of observations from the

individual threshold method. The average plot voltages and number of points above the individual threshold were multiplied to find area above the curve for each plot. This area above the curve was then plotted against chlorophyll concentration and content.

Method	Method Name	Description
1	Whole Plot Average Voltage	Average all voltage readings in the plot
2	Plant Plot Average Voltage (Exemplary Method)	Average voltage readings taken only over plant biomass
3	Fixed Threshold	Average voltage readings above a single threshold applied to all plots
4	Individual Threshold	Average voltage readings above threshold selected for each plot
5	Area Above Fixed Threshold	Average voltage above fixed threshold (method 3) multiplied by the number of readings above the fixed threshold
6	Area Above Individual Threshold	Ave V above individual threshold (method 4) multiplied by number of readings above individual threshold

Table 3. Summary of active sensor data processing methods.

Results and Discussion

This study focused on the estimation of chlorophyll concentration in spinach. Estimates of biomass and chlorophyll content were based on information from digital images and the passive sensor. Chlorophyll concentration estimates were also made from the readings of the active sensor. These readings were manipulated with six different methods to investigate if nitrogen concentration could be estimated from the Patchen sensor data.

The objective of this study was to determine a method of estimating chlorophyll concentration by utilizing data from %VC (vegetative cover), the passive sensor, and the

active sensor. An initial examination of the %VC and NDVI data showed there was a significant correlation between %VC and dry biomass, and in addition a significant correlation between NDVI and chlorophyll content. The correlation between %VC and dry biomass was $r^2 = 0.731$ for fall 2000 and $r^2 = 0.979$ for spring 2001 as shown in Figure 11. Spring 2001 readings from the passive sensor produced a correlation between NDVI and chlorophyll content of $r^2 = 0.887$ and between NDVI and chlorophyll concentration of $r^2 = 0.743$.

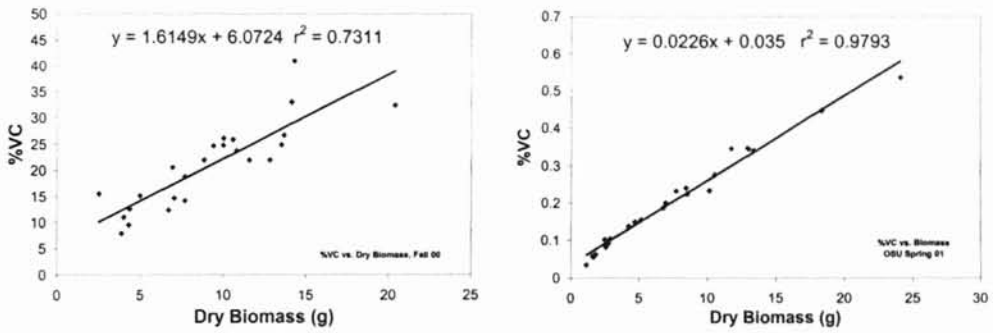

Figure 11. Graph showing relation between %VC and biomass for Fall 2000 and Spring 2001.

Two different approaches were used to estimate chlorophyll concentration from the information provided by the %VC and the passive sensor NDVI readings. The first method utilized estimates of biomass produced by the %VC correlations and chlorophyll content estimates produced by the NDVI correlations. The chlorophyll content estimate was divided by the biomass estimate providing an estimate of chlorophyll concentration (Equation 7). Equation 8 shows the dimensional logic for this method.

$$\frac{chlorophyll \quad content \quad estimation}{biomass \quad estimate} = chlorophyll \quad concentration \quad estimate \quad (7)$$

$$\frac{mg \quad chlorophyll}{kg \quad spinach \quad biomass} = mg/kg \quad chlorophyll \quad concentration \qquad (8)$$

These estimates of chlorophyll were graphed against the chlorophyll concentration measurements with little correlation (r^2= 0.303).

NDVI is highly correlated with chlorophyll content and %VC is highly correlated with dry biomass. With this in mind, the second approach divided the NDVI readings by the %VC calculations, and the results were plotted against measured chlorophyll concentration. The results provided low correlation (r^2 = 0.385). Graphs of the passive sensor chlorophyll concentration estimates may be found in Appendix B.

Data from the active sensor were then examined. As discussed previously, the voltage from the Patchen sensor is related to NDVI. The average voltage reading of each plot was graphed against chlorophyll content and concentration, as shown in Figure 12.

A summary of results for the six data processing methods for active sensor voltage data may be seen in Table 4. The correlation between whole plot average voltage readings and chlorophyll content was r^2 = 0.805. Correlation between whole plot average voltage and chlorophyll concentration was r^2 = 0.699. The plant plot average voltage produced a slightly increased correlation (r^2 = 0.711). The fixed threshold (r^2 = 0.699) produced results equal to the whole plot average voltage with the individual threshold (r^2 = 0.512), area above fixed threshold (r^2 =0.518), and area above individual threshold (r^2 = 0.530) producing results with lower correlations. Graphs may be found in Appendix C.

Method	Method Name	Correlation (r^2) of Patchen Voltage to Chlorophyll Concentration
1	Whole Plot Average Voltage	0.699
2	Plant Plot Average Voltage (Exemplary Method)	0.711
3	Fixed Threshold	0.699
4	Individual Threshold	0.512
5	Area Above Fixed Threshold	0.518
6	Area Above Individual Threshold	0.530

Table 4. Correlation between voltage and chlorophyll concentration for active sensor readings.

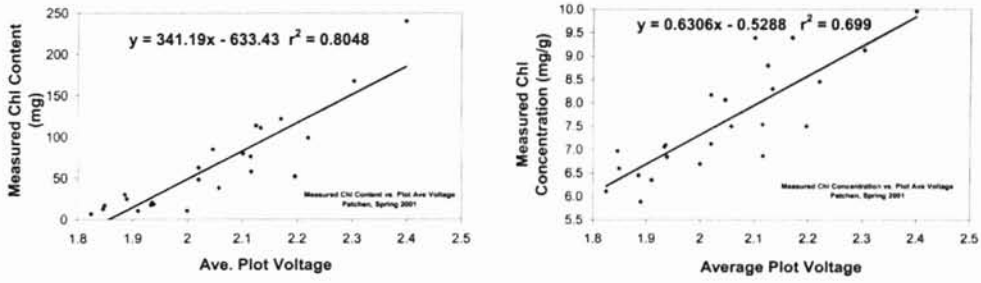

Figure 12. Graph relating active sensor readings to chlorophyll content and concentration.

Conclusion

The best correlations for estimating chlorophyll concentration were found with the simple correlations to NDVI. No significant correlations were found with methods

which divided chlorophyll content estimators by biomass estimators, nor were any improvements in correlation found between manipulated active sensor voltage values and chlorophyll concentration. The highest correlation for chlorophyll concentration was found to be with the NDVI readings from the passive sensor ($r^2 = 0.887$). The next best correlation was with the voltage readings from the active sensor using the plant plot average voltage with an $r^2 = 0.711$. The effort required for this method was not worth the small increase in correlation over that found between the direct active sensor voltage and chlorophyll concentration ($r^2 = 0.699$). Methods of estimating chlorophyll concentration by dividing estimates from the passive sensor and %VC provided lower correlations ($r^2 = 0.303$ and $r^2 = 0.385$). Estimates with data from the active sensor were also poor, ranging from $r^2 = 0.512$ to 0.711.

This study reaffirmed the correlation between %VC and dry biomass found by Lukina et al. (1999, 2000) and Ter-Mikaelian and Parker (2000). High correlation ($r^2 = 0.979$ for fall 2000 and $r^2 = 0.731$ for spring 2001) was observed between the %VC of the spinach and the spinach dry biomass. The findings of Lukina et al. (1999, 2000) and Sembiring (1998) were also supported, regarding NDVI readings producing a more accurate estimate of chlorophyll content than of chlorophyll concentration.

References

Adamsen, F. J., T. A. Coffelt, J. M. Nelson, E. M Barnes, and R. C. Rice. 2000. Crop ecology, management & quality. *Crop Sci.*, 40: 704-709.

Beck, J. 1996. Reduced herbicide usage in perennial crops, row crops, fallow land and non-agricultural applications using optoelectronic detection. SAE Paper No. 96-1758. Indianapolis, Indiana: SAE.

Birth, G. S. and G. R. McVey. 1968. Measuring the color of growing turf with a reflectance spectrophotometer. *Agron. J.* 60: 640-643.

Carlson, T. N. and D. A. Ripley. 1997. On the relation between NDVI, fractional vegetation cover, and leaf area index. *Remote Sens. Environ.* 62: 241-252.

Chancellor, W. J. and M. A. Goronea. 1994. Effects of spatial variability of nitrogen, moisture, and weeds on the advantages of site-specific applications for wheat. *Trans. ASAE* 37(3): 717-724.

Inskeep, W. P. and P. R. Bloom. 1985. Extinction coefficients of chlorophyll *a* and *b* in N, N-Dimethylformamide and 80% Acetone. *Plant Physiol.* 77: 483-485.

Jensen, J. R. 2000. *Remote Sensing of the Environment: an Earth Resource Perspective.* Upper Saddle River, N.J.: Prentice Hall.

Lukina, E. V., M. L. Stone, and W. R. Raun. 1999. Estimating vegetation coverage in wheat using digital images. *J. Plant Nutr.* 22(2): 341-350.

Lukina, E. V., W. R. Raun, M. L. Stone, J. B. Solie, G. B. Johnson, H. L. Lees, J. M. LaRuffa, and S. B. Phillips. 2000. Effect of row spacing, growth stage, and nitrogen rate on spectral irradiance in winter wheat. *J. Plant Nutr.* 23(1): 103-122.

Merritt, S. J., K. Von Bargen, G. E. Meyer, and D. A. Mortensen. 1994. Reflectance sensor and control system for spot spraying. ASAE Paper No. 94-1057. St. Joseph, Mich.: ASAE.

Moorby, J. and R. T. Besford. 1983. Mineral nutrition and growth. In *Encyclopedia of Plant Physiology New Series, V15b*, ed. A. Lauchi and R. L. Bieleski, 481-529. Berlin, Springer-Verlag.

Munden, R., P. J. Curran, and J. A. Catt. 1994. The relationship between red edge and chlorophyll concentration in the Broadbalk winter wheat experiment at Rothamsted. *Int. J. Remote Sens.* 15(3): 705-709.

Needham, D. L. 2002. Personal communication with author. Stillwater, OK, 15 April.

Pinter, P. J. Jr. 1993. Solar angle independence in the relationship between absorbed PAR and remotely sensed data for alfalfa. *Remote Sens. Environ.* 46: 19-25.

Pinter, P. J. Jr., H. L. Kelly Jr., and S. Schnell. 1987. Spectral estimation of alfalfa biomass under conditions of variable cloud cover. In *8th Conference on Biometeorology and Aerobiology*. Boston, MA., American Meteorological Society, Boston Mass., Sept 14-18.

Pinter, P. J. Jr., R. D. Jackson, and S. M. Moran. 1990. Bidirectional reflectance factors of agricultural targets: a comparison of ground-, aircraft-, and satellite-based observations. *Remote Sens. Environ.* 32:215-228.

Raun, W. R., J. B. Solie, G. V. Johnson, M. L. Stone, R. W. Whitney, H. L. Lees, H. Sembiring, and S. B. Phillips. 1998a. Microvariability in soil test, plant nutrient, and yield parameters in bermudagrass. *Soil Sci. Soc. Am. J.* 62(3): 683-690.

Raun, W. R., G. V. Johnson, H. Sembiring, E. V. Lukina, J. M. LaRuffa, W. E. Thomason, S. B. Phillips, J. B. Solie, M. L. Stone, and R. W. Whitney. 1998b. Indirect measures of plant nutrients. *Commun. Soil Sci. Plant Anal.* 29(11-14): 1571-1581.

Rouse, J. W., R. H. Hass, J. A. Schell, D. W. Deering, and J. C. Harlan. 1974. Monitoring the vernal advancement of retrogradation of natural vegetation. NASA/GSFC, Type III, Final Report. Greenbelt, MD.

Sawyer, J. E. 1994. Concepts of variable rate technology with considerations for fertilizer application. *J. Prod. Agric.* 7(2): 195-201.

Sembiring, H., W. R. Raun, G. V. Johnson, M. L. Stone, J. B. Solie, and S. B. Phillips. 1998. Detection of nitrogen and phosphorus nutrient status in winter wheat using spectral radiance. *J. Plant Nutr.* 21(6): 1207-1233.

Solie, J. B., W. R. Raun, R. W. Whitney, M. L. Stone, and J. D. Ringer. 1996. Optical sensor based field element size and sensing strategy for nitrogen application. *Trans. ASAE* 39(6): 1983-1992.

Stone, M. L., J. B. Solie, W. R. Raun, R. W. Whitney, S. L. Taylor, and J. D. Ringer. 1996a. Use of spectral radiance for correcting in-season fertilizer nitrogen deficiencies in winter wheat. *Trans. ASAE* 39(5):1623-1631.

Stone, M. L., J. B. Solie, R. W. Whitney, W. R. Raun, and H. L. Lees. 1996b. Sensors for detection of nitrogen in winter wheat. ASAE Paper No. 96-1757. St. Joseph, Mich.: ASAE.

Ter-Mikaelian, M. T. and W. C. Parker. 2000. Estimating biomass of white spruce seedlings with vertical photo imagery. *New Forests* 20: 145-162.

Thiam, A. K. 1998. Geographic information systems and remote sensing methods for assessing and monitoring land degradation in the Sahel region: the case of southern Mauritania. Ph.D. Dissertation. Clark University, Worcester, MA., USA.

Wood, C. W., D. W. Reeves, R. R. Duffield, and K. L. Edmisten. 1992. Field chlorophyll measurements for evaluation of corn nitrogen status. *J. Plant Nutr.* 15(4): 487-500.

APPENDICES

APPENDIX A

FALL 2000 PLOT LAYOUT

Figure A. 1 Fall 2000 plot layout.

SPRING 2001 PLOT LAYOUT

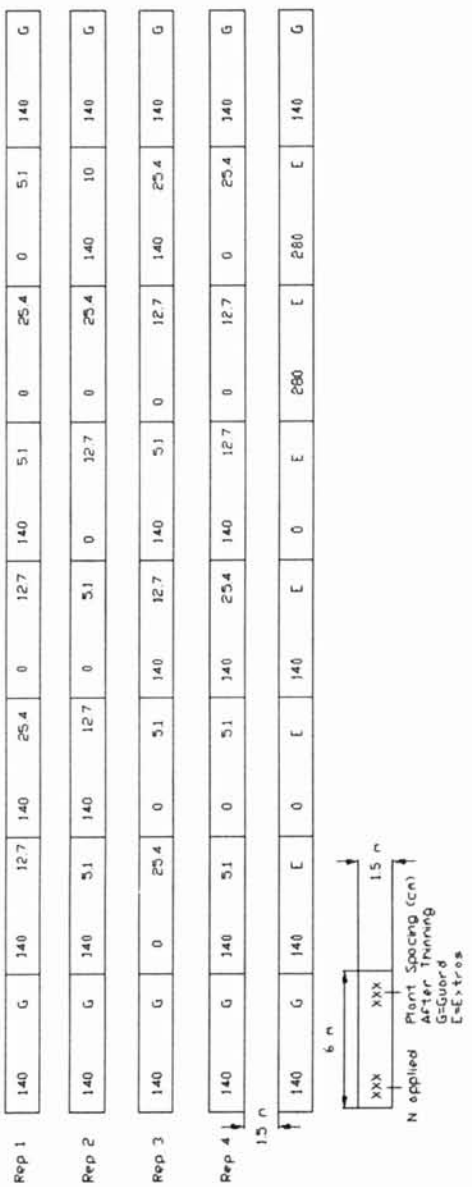

Figure A. 2 Spring 2001 plot layout.

APPENDIX B

OSU REFLECTANCE SENSOR DATA GRAPHS

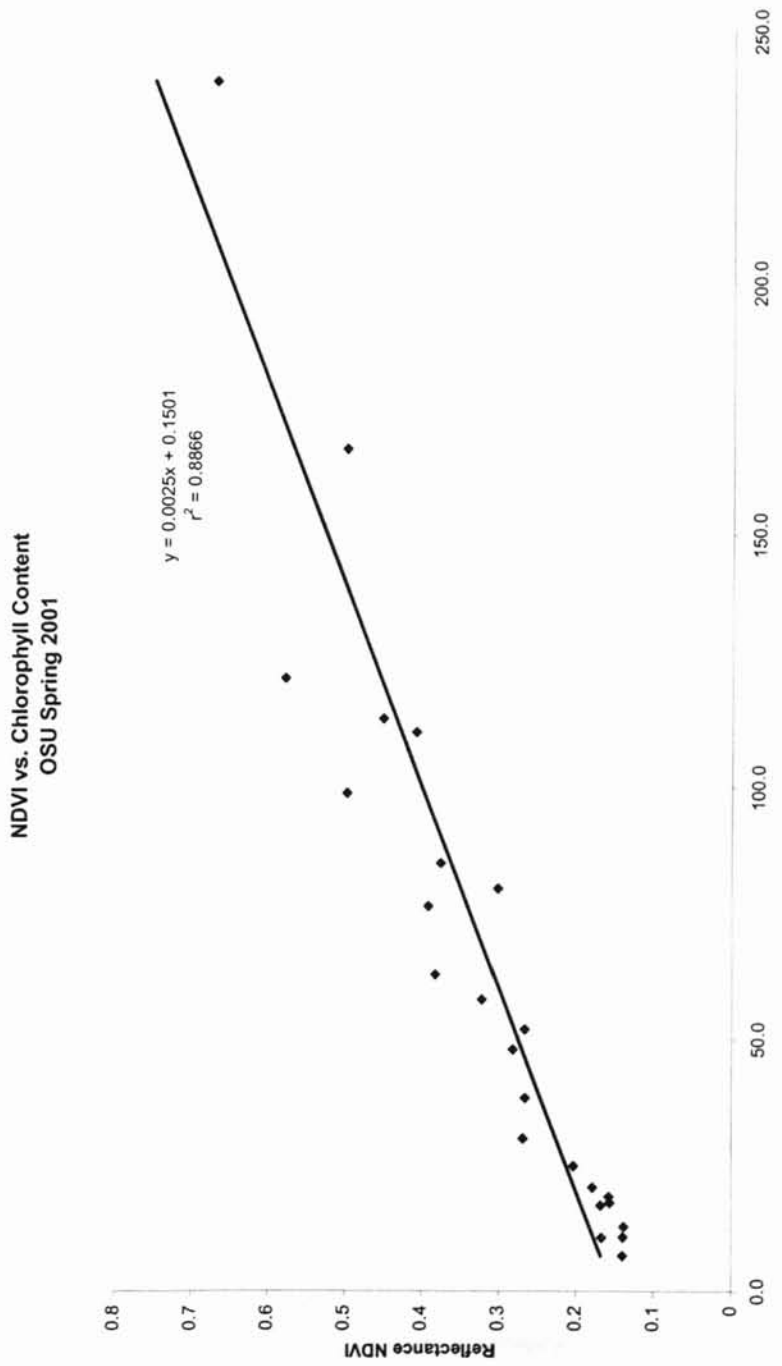

Figure B. 1 Reflectance NDVI vs. chlorophyll content (OSU Sensor, Spring 2001).

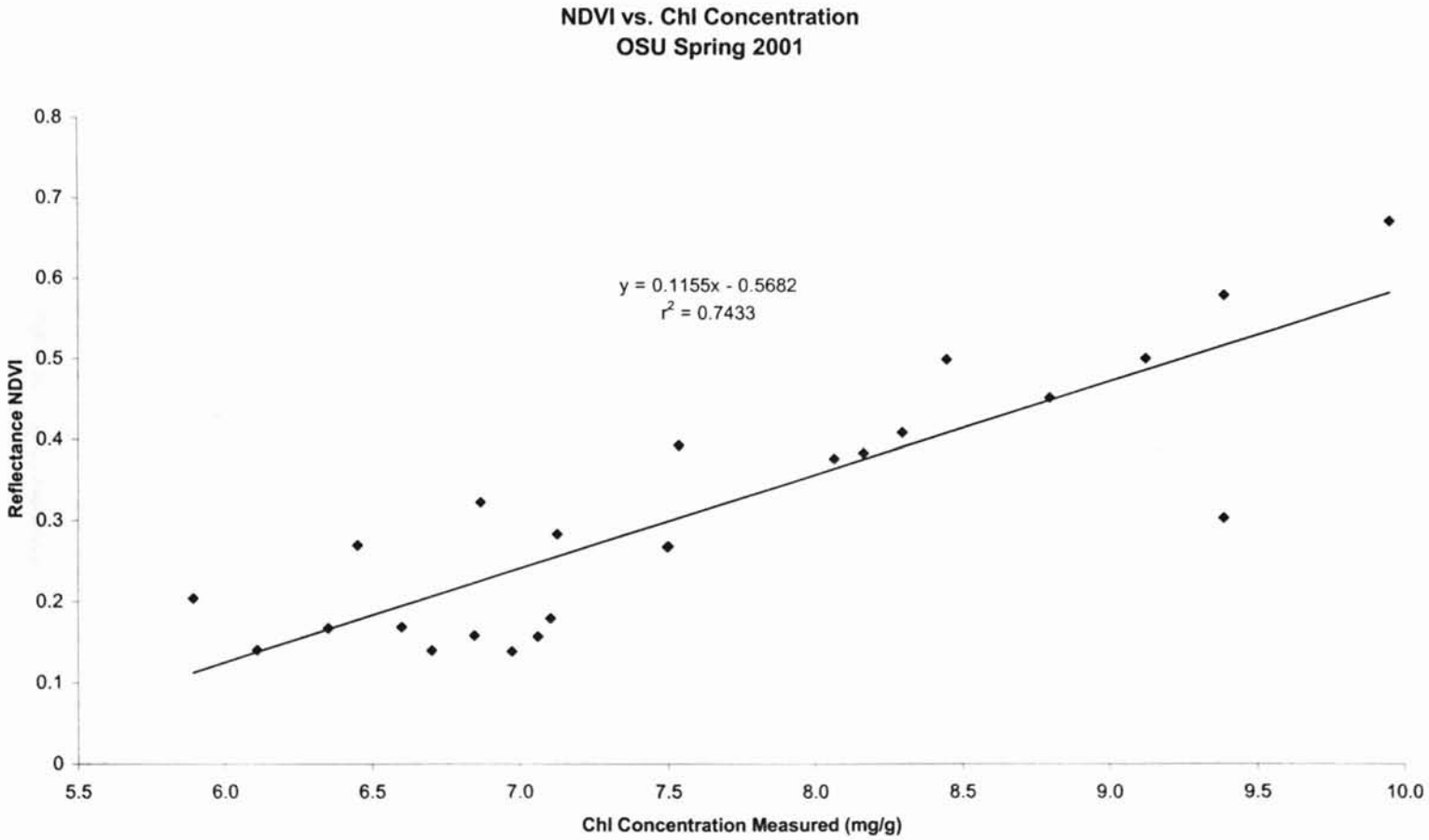

Figure B. 2 Reflectance NDVI vs. chlorophyll concentration (OSU Sensor, Spring 2001).

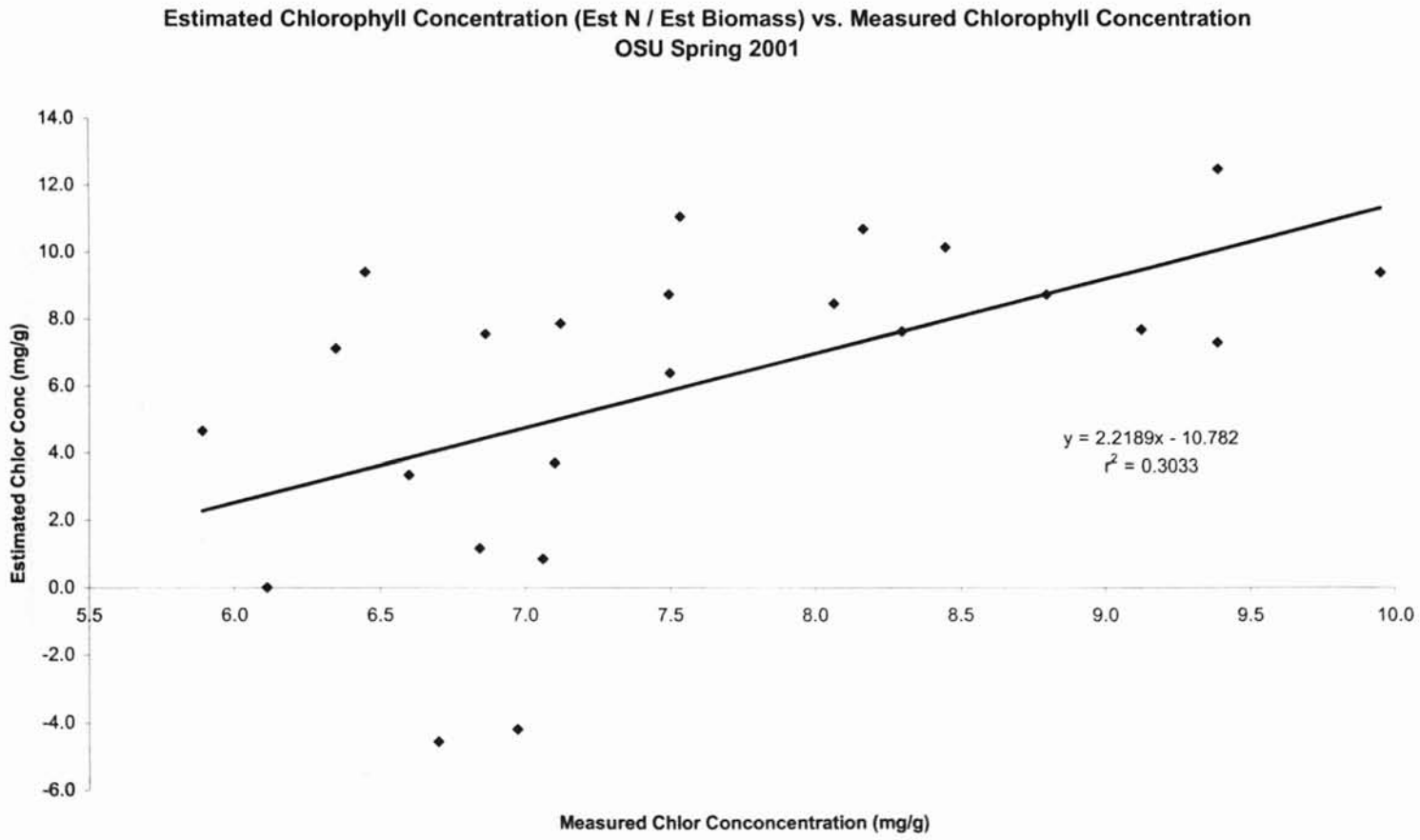

Figure B. 3 Estimated chlorophyll concentration (est N / est biomass) vs. measured chlorophyll concentration (OSU Sensor, Spring 2001)

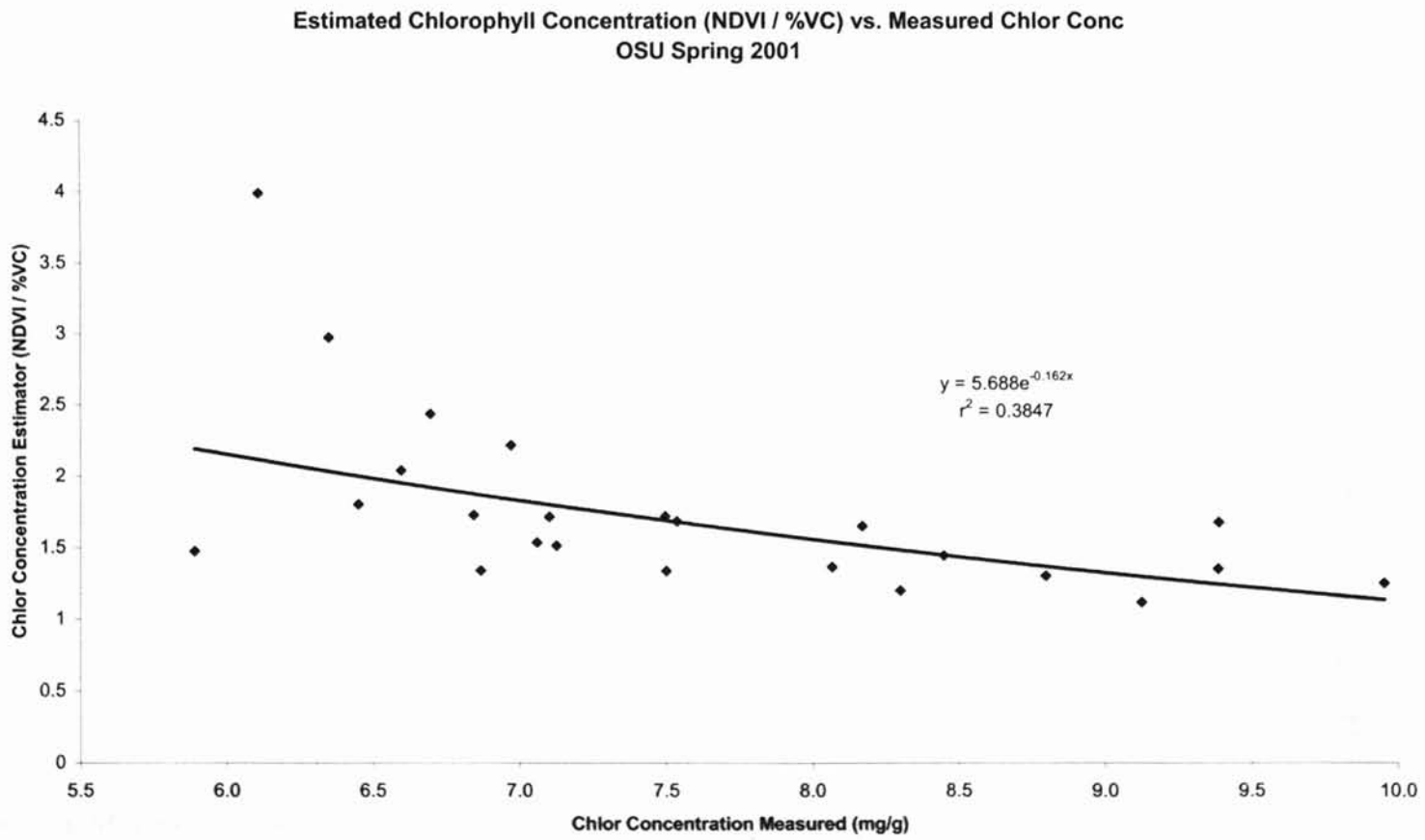

Figure B. 4 Estimated chlorophyll concentration (NDVI / %VC) vs. measured chlorophyll concentration (OSU Sensor, Spring 2001).

APPENDIX C

PATCHEN DATA GRAPHS

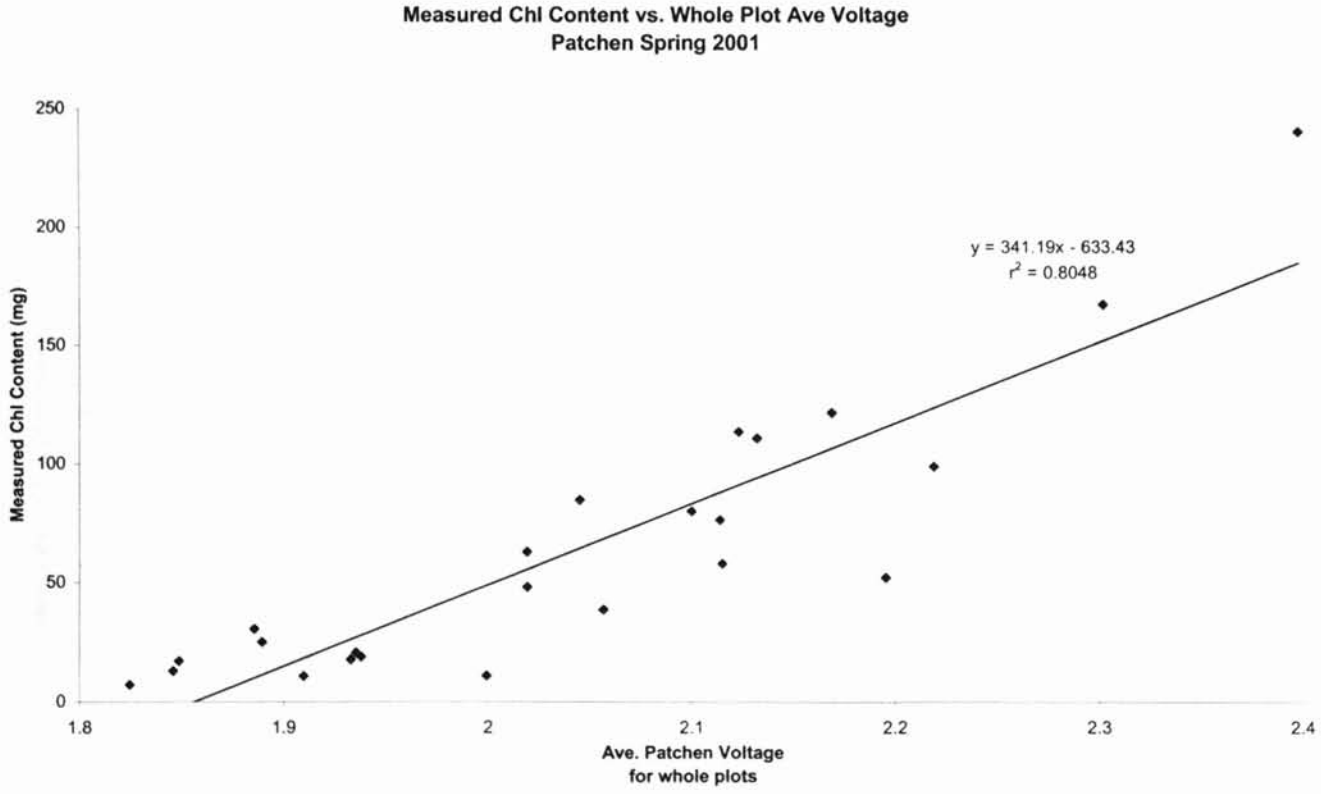

Figure C. 1 Measured chlorophyll content vs. whole plot average voltage (Patchen, Spring 2001).

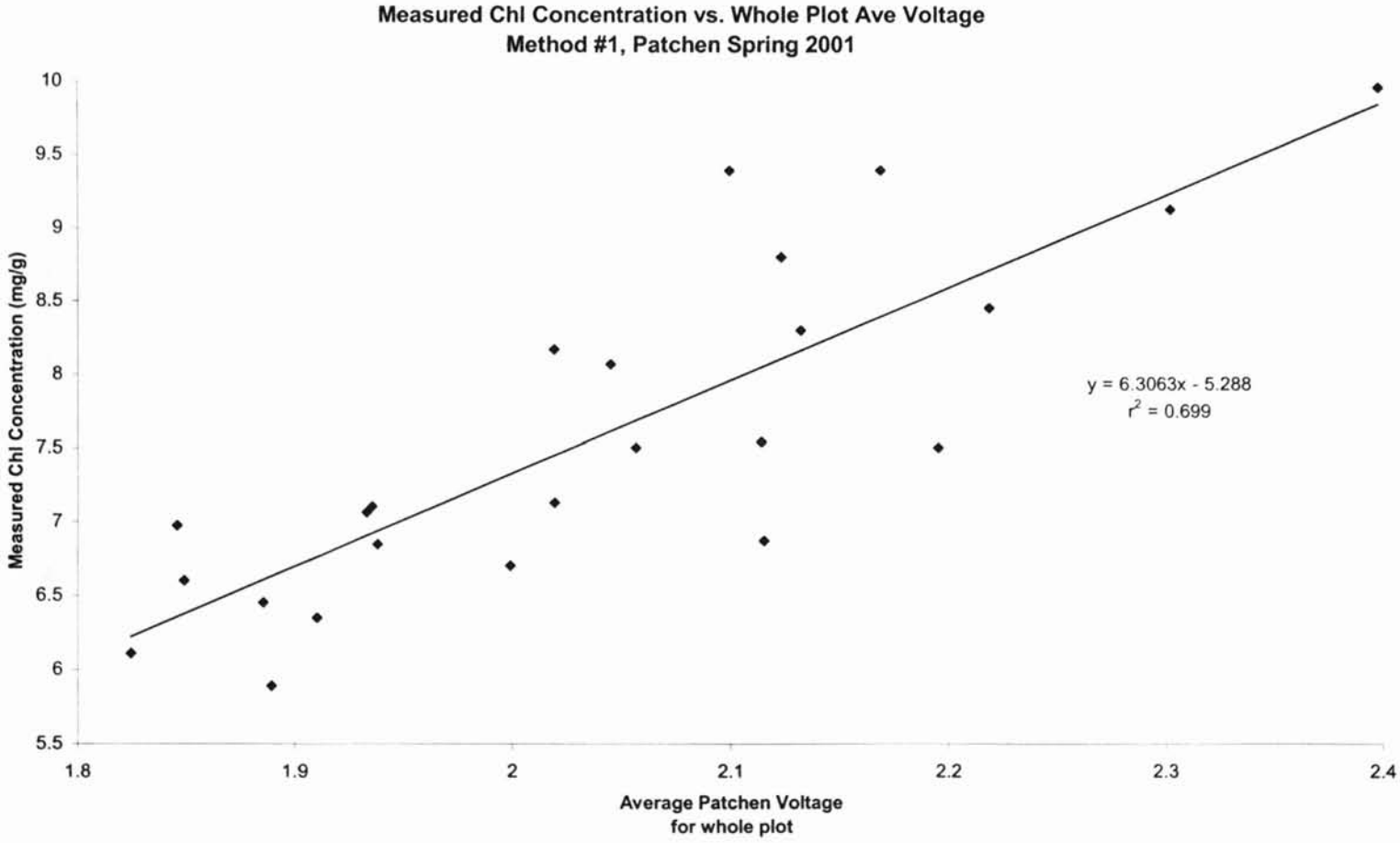

Figure C. 2 Method #1, Measured chlorophyll concentration vs. whole plot average voltage (Patchen, Spring 2001).

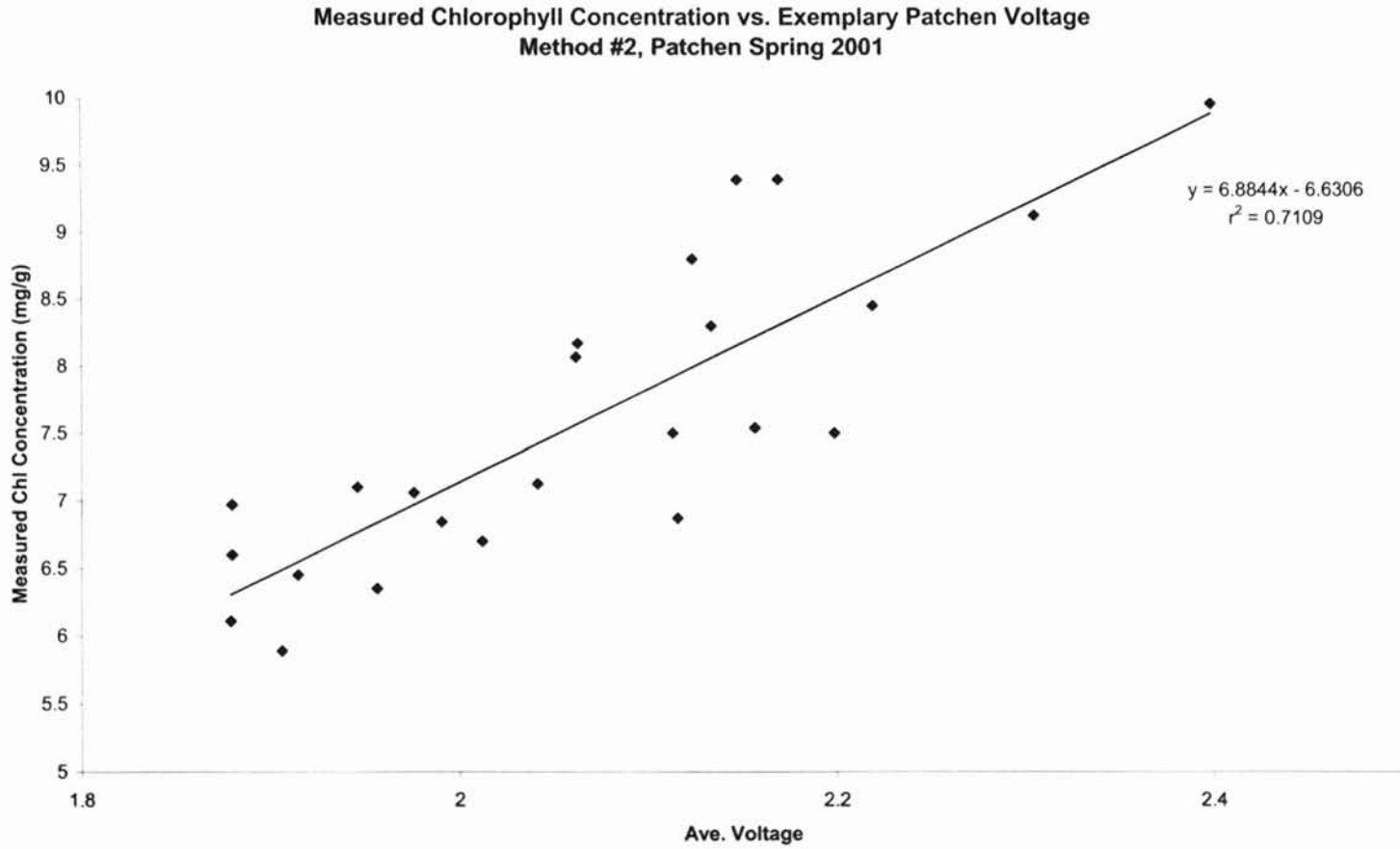

Figure C. 3 Method 2, Measured chlorophyll concentration vs. exemplary Patchen voltage (Patchen, Spring 2001).

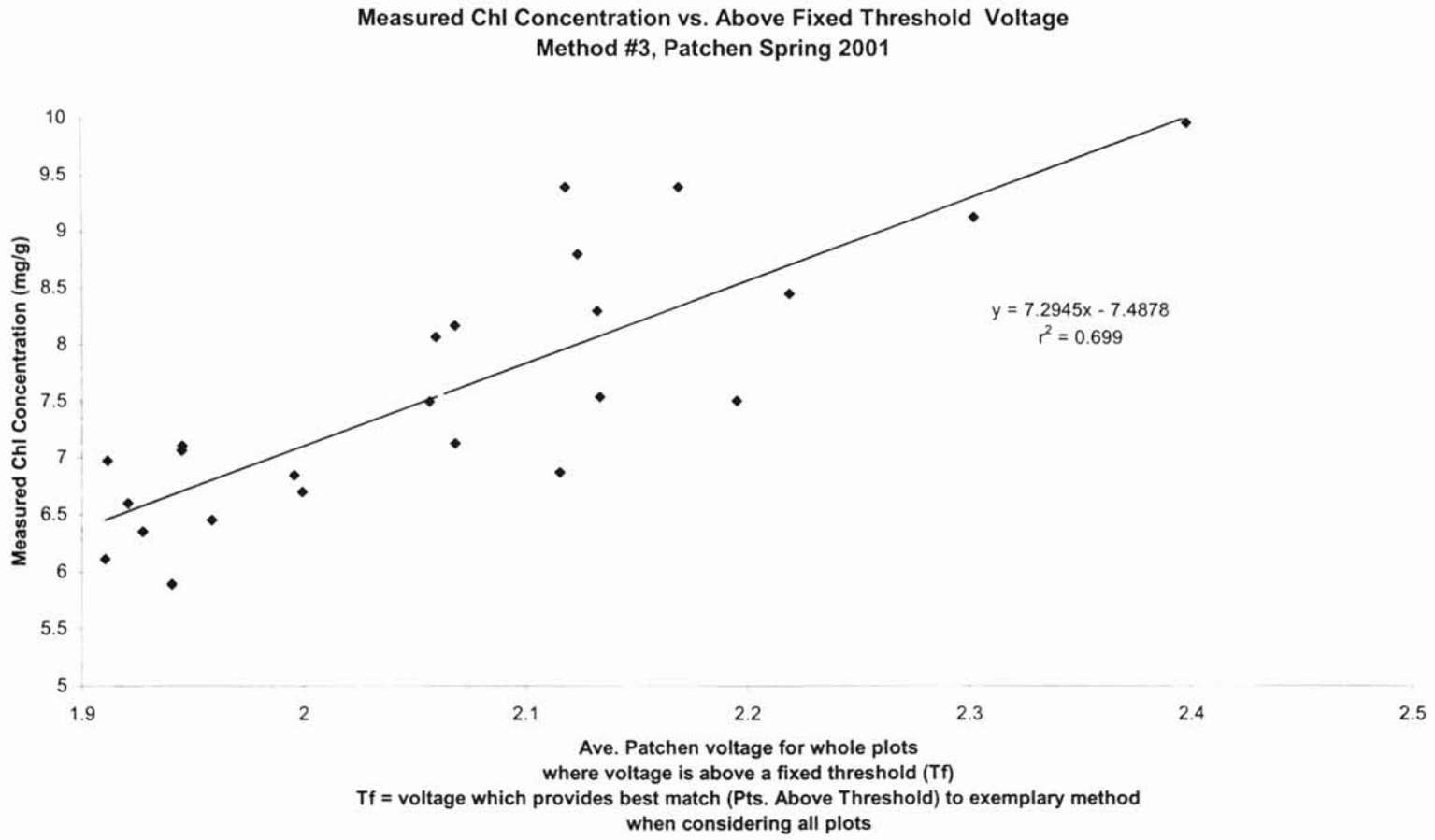

Figure C. 4 Method 3, Measured chlorophyll concentration vs. above fixed threshold voltage (Patchen, Spring 2001).

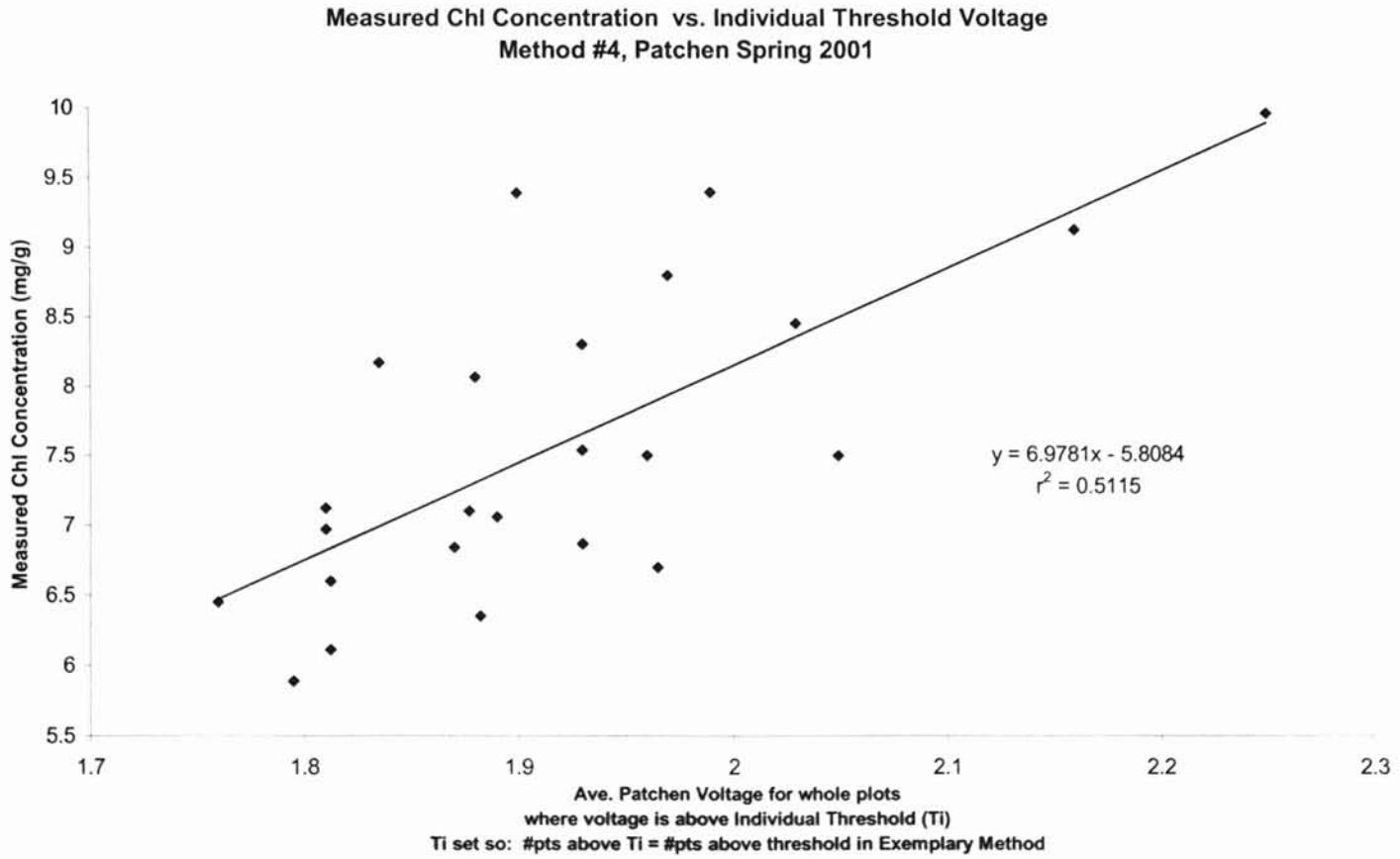

Figure C. 5 Method 4, Measured chlorophyll concentration vs. individual threshold voltage (Patchen, Spring 2001).

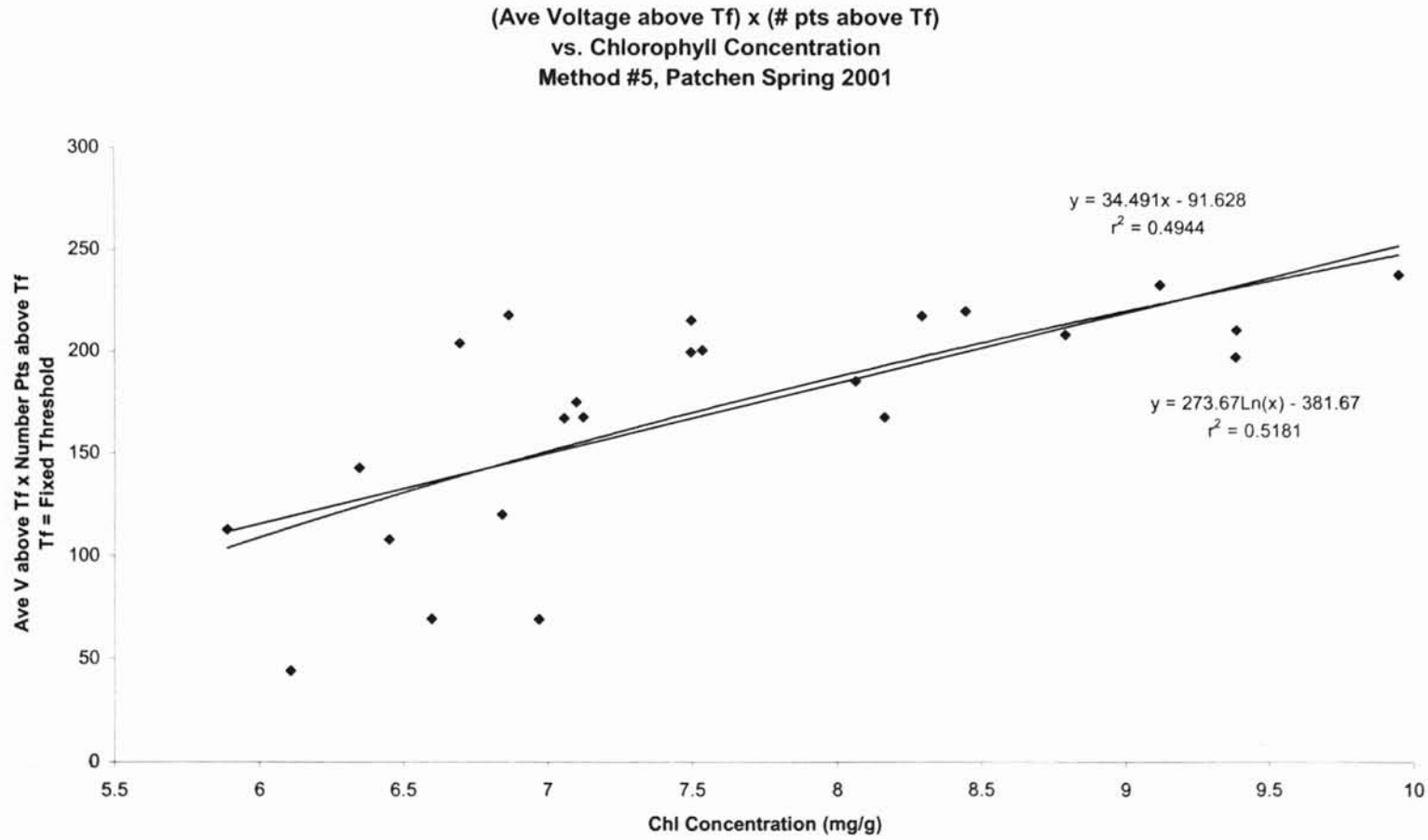

Figure C. 6 Method 5, (ave voltage above Tf) x (#pts above Tf) vs. chlorophyll concentration (Patchen, Spring 2001).

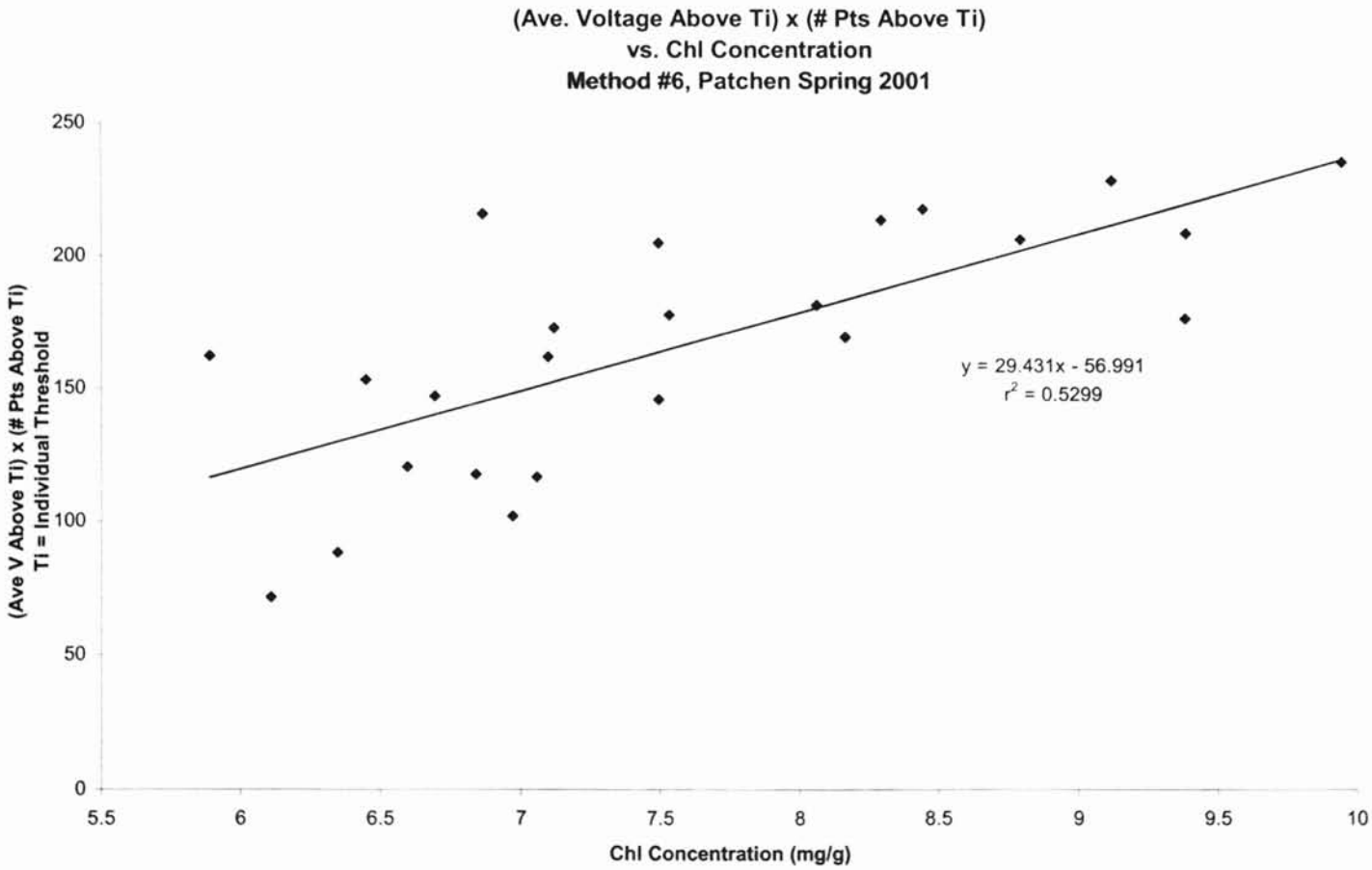

Figure C. 7 Method 6, (ave. voltage above Ti) x (# pts above Ti) vs. chlorophyll concentration (Patchen, Spring 2001)

VITA 2

Theodore D. Kersten

Candidate for the Degree of

Master of Science

Thesis: REMOTE SENSING BASED METHOD FOR ESTIMATING CHLOROPHYLL CONCENTRATION IN SPINACH

Major Field: Biosystems Engineering

Biographical:

Personal Data: Born in Escondido, California on October 9, 1970, the son of Daniel D. and Betty G. Kersten.

Education: Graduated from Orange Glen High School, Escondido, California, June 1989; received a Bachelor of Science degree in Biosystems and Agricultural Engineering for the California Polytechnic State University - San Luis Obispo, California, June, 1999; received a Bachelor of Science degree in Business Administration, Marketing from the California Polytechnic State University – San Luis Obispo, California, June, 1999; completed the requirements for the Master of Science Degree with a major in Biosystems Engineering from Oklahoma State University, August, 2002.

Professional Experience: Graduate Assistant, Biosystems and Agricultural Engineering Department, Oklahoma State University, August, 1999 to May, 2002.